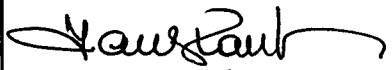



1. Publication N ^o <i>INPE-2367-RA/161</i>	2. Version	3. Date <i>April, 1982</i>	5. Distribution <input type="checkbox"/> Internal <input checked="" type="checkbox"/> External <input type="checkbox"/> Restricted
4. Origin <i>DGA/DIG</i>			Program <i>MATE</i>
6. Key words - selected by the author(s) <i>GEOMAGNETIC VARIATIONS</i> <i>STORM-TIME CHANGES</i>			
7. U.D.C.: <i>550.38</i>			
8. Title <i>COMPARISON OF STORM-TIME CHANGES OF GEOMAGNETIC FIELD AT GROUND AND AT MAGSAT ALTITUDES PART II</i>			10. N ^o of pages: <i>41</i>
			11. Last page: <i>40</i>
			12. Revised by
9. Authorship <i>Rajaram Purushottam Kane</i> <i>Nalin Babulal Trivedi</i>			 <i>Ivan Jelinek Kantor</i>
Responsible author <i>Rajaram P. Kane</i>			13. Authorized by  <i>Nelson de Jesus Parada</i> Director
14. Abstract/Notes <i>The study of ΔH_O(Dawn) and ΔH_O(Dusk) was extended to the whole period Nov. 2, 1979 - Jan. 18, 1980, involving about 1200 Dawn and 1200 Dusk passes. Quiet-time base values for 5° longitude belts were estimated. After subtracting these from the observed values, the residual ΔH_O(Dawn) and ΔH_O(Dusk) were studied for the two major storms of Nov. 11-15, 1979 and Dec. 31, 1979 - Jan. 2, 1980. It was noticed that ΔH_O(Dusk) attained larger (negative) values and for a longer time, than ΔH_O(Dawn). Some changes in ΔY_O and ΔZ_O were also noticed, indicating possibilities of either meridional currents and/or noncoincidence of the central plane of the ring current with the equatorial plane of the earth. Other details are described.</i>			
15. Remarks			

2nd MAGSAT Progress Report for Project M55 - April 1982

COMPARISON OF STORM-TIME CHANGES OF GEOMAGNETIC FIELD
AT GROUND AND AT MAGSAT ALTITUDES
PART II

Rajaram Purushottam Kane and Nalin Babulal Trivedi

Instituto de Pesquisas Espaciais - INPE
Conselho Nacional de Desenvolvimento Científico e Tecnológico - CNPq
12200 - São José dos Campos, S.P., Brazil

1. Introduction

The purpose of the present investigation is to study the storm-time variations observed at MAGSAT altitudes and compare these with similar variations observed at ground.

2. Techniques

In the previous report, it was mentioned that the parameter we chose for study of the variations at MAGSAT altitudes was $\Delta H = H(\text{observed}) - H(\text{Model})$, where $H = (X^2 + Y^2 + Z^2)^{1/2}$ where X, Y, Z are the components actually observed. Since the MAGSAT altitude is not constant but varies roughly in a geocentric radius range of $R = 6800 \pm 100$ km, the ΔH values were normalised to a constant geocentric distance of 6800 km by using an inverse R^3 relationship.

For every day commencing from Nov. 2, 1979, there were roughly 15 Dawn passes and 15 Dusk passes, interlaced alternatively. Thus equatorial crossings of consecutive Dawn and Dusk passes were roughly 0.8 hours apart while consecutive Dawn passes (or Dusk passes) had equatorial crossings roughly 1.6 hours apart. In the previous

report, ΔH_0 (Dawn) and ΔH_0 (Dusk) plots (i.e. ΔH for equator) for the first 18 days viz. Nov. 2-19, 1979 were demonstrated. Here, we examine similar data for an extended period of 78 days, viz. Nov. 2, 1979 - Jan. 18, 1980.

3. Accomplishments

Figs 1-6 show the plots of ΔH_0 (Dawn), as dots and full lines, ΔH_0 (Dusk) as dashes and crosses, Dst (full lines) and K_p (histograms). The following may be noted:

- (1) Both the ΔH_0 (Dawn) and ΔH_0 (Dusk) seem to show variations similar to Dst. In the interval of 78 days, there seem to have occurred two major storms, one during Nov. 11-16, 1979 (Fig.1) and another during Jan 1-3, 1980 (Fig.5) and several minor storms; during Nov. 7-8, 1979 (Fig.1), Nov. 24-25, 1979 (Fig.2), Dec 3-5, 1979 (Fig.3), Dec 28-30, 1979 (Fig.5) and Jan 13-14, 1980 (Fig.6).
- (2) Even in quiet periods, ΔH_0 (Dawn) and ΔH_0 (Dusk) are different from zero, usually negative, and, unequal to each other. In disturbed periods, ΔH_0 (Dusk) is invariably larger negative than ΔH_0 (Dawn). Since the Dusk and Dawn passes occur only alternatively, at a spacing of about 0.8 hours, a direct comparison of observed ΔH_0 (Dawn) and ΔH_0 (Dusk) is not possible. However, as outlined in Table 1 of the first report (reproduced here also as Table 1) the average of two successive Dawn (Dusk) passes could be considered as simultaneous in time with the Dusk (Dawn) pass that occurred in between. For a comparative study, ΔH_0 i.e. the values of ΔH for equatorial region for the first few days of November 1979 were considered. Data for Nov. 2 seemed to be faulty and were omitted. Fig. 7 shows the results.

In Fig. 7(a), we plot ΔH_0 (Dusk) versus ΔH_0 (Dawn) for Nov. 3-5, 1979. This period was only moderately disturbed, with Dst

within -35 nT. The scatter of points in Fig.7(a) is rather large. The correlation coefficient for 87 pairs of points is only $(+0.42 \pm 0.09)$ and the two regression lines, one with ΔH_0 (Dusk) as independent variable (full line) and the other with ΔH_0 (Dawn) as independent variable (dashed line) are wide apart and make different intercepts on the two axes. Part of the scatter could be because, not only observed values of ΔH_0 but averages of successive values have been used. However, we expect the error on this count to be only about ± 5 nT, specially during moderately disturbed periods. The scatter in Fig.7(a) is beyond these limits.

Fig.7(b) shows a similar plot for the next 4 days viz. Nov. 6-10, 1979. This is a mildly disturbed period with Dst reaching -40 nT. Here, some points (marked as crosses) seem to be widely away from the other points (dots) which seem to fall on a reasonably good straight line. In Fig.7(b), the upper regression line is for the dots only which represent 89 values and the correlation coefficient is $(+0.91 \pm 0.02)$. The lower regression line is for dots and crosses together (total 153 values) and the correlation coefficient is only $(+0.71 \pm 0.04)$. The crosses represent large negative values of ΔH_0 (Dusk) which are not accompanied by large ΔH_0 (Dawn) and thus, could be either erroneous and/or might represent some aspect of storm-time variation confined mainly to the dusk quadrant.

Fig.7(c) shows a similar plot for the storm period Nov. 11-15, 1979. Here the recovery period Nov. 14-15 is marked as crosses. Two separate regression lines are indicated, one for the main storm (Nov. 11, 12, 13) of slope exceeding unity and another for the recovery period (Nov. 14, 15) of slope almost unity. It seems obvious, that the evolutions of ΔH_0 (Dawn) and ΔH_0 (Dusk) are different in the two phases of the storm (main phase and recovery). We will discuss this again later.

Fig.7(d) represents the period Nov. 16-20, 1979 which is essentially quiet, except on Nov. 16 when Dst was near -35 nT

for a few hours. The scatter is quite large. The correlation coefficient is $(+ 0.64 \pm 0.05)$ and the two regression lines, one with $\Delta H_0(\text{Dusk})$ as independent variable (full line) and the other with $\Delta H_0(\text{Dawn})$ as independent variable (dashed line) are widely apart.

It seems from Fig.7 that there is a possibility that the storm-time evolution of $\Delta H_0(\text{Dawn})$ and $\Delta H_0(\text{Dusk})$ is different from each other; but the scatter even in quiet periods indicates considerable pollution in the values of both these parameters.

What could be the source of such a pollution? Apart from the possibility that the basic data may have possible errors of a few nT, two possibilities arise:

- (a) Sugiura and Hagan (1979) have indicated that the Sq effect even at MAGSAT altitudes and even at Dusk and Dawn periods may not be negligible. Thus, $\Delta H_0(\text{Dawn})$ and $\Delta H_0(\text{Dusk})$ may differ on this count, even during quiet or moderately disturbed periods.
- (b) The values used so far are for varying longitudinal belts. Thus, effects due to local ground anomalies may be present.

If these effects do exist, these should be estimated and subtracted from the $\Delta H_0(\text{Dusk})$ and $\Delta H_0(\text{Dawn})$ values so that storm effects in the two can be properly studied. For this purpose, ΔH_0 values for about 1200 Dawn passes and 1200 Dusk passes (for the 78 days data) were separated into 72 longitudes groups viz. -180° to -175° , -5° to 0° , 0° to $+5^\circ$ $+175^\circ$ to $+180^\circ$; and, for each 5° longitude group, the $\Delta H_0(\text{Dawn})$ and $\Delta H_0(\text{Dusk})$ were plotted separately versus Dst. Fig.8(a), left half, shows the plot of $\Delta H_0(\text{Dawn})$ versus Dst and the right half shows $\Delta H_0(\text{Dusk})$ versus Dst, for the longitude belt 0° to $+5^\circ$. The 1200 passes of each type (Dawn or Dusk) are distributed roughly equally in the 72 longitude groups and hence, each group has roughly 15 pairs of ΔH_0 and Dst values. The correlation coefficients are reasonably high (about $+ 0.80$ or more) and the lines

drawn are the regression lines with ΔH_0 as the independent parameter. Here, it is not the value of the slope that is important; but it is the intercept on the ΔH_0 axis which we are seeking, as it gives the base value of ΔH_0 for quiet conditions (Dst=0). Thus, for the longitude belt 0° to 5° , ΔH_0 (Dawn) had a base value of - 26 nT and ΔH_0 (Dusk) was - 40 nT. These values, with errors of about ± 2 nT, are different from zero, probably indicating that the model values of H have missed systematic ground anomaly effects of this order. Also, ΔH_0 (Dusk) and ΔH_0 (Dawn) are different, probably indicating the magnitude of the difference in the Dawn and Dusk Sq effect at equator for this longitude belt.

Fig.8(b) shows similar plots for the longitude belts $+5^\circ$ to $+10^\circ$. Fig.9(a) shows results for longitude $+10^\circ$ to $+15^\circ$ and Fig.9(b) for $+15^\circ$ to $+20^\circ$. In almost all the cases, correlation coefficients exceeded + 0.70 and the intercepts on ΔH_0 axis were invariably negative. Plots for other longitudes are not shown here. The values of the intercepts are plotted versus longitude in Fig.10 and given in Table 2. The uppermost row (first row, Fig.10) shows ΔH_0 (Dusk) versus longitude. The intercept values range from - 24 nT to - 41 nT for the geographical equatorial region. These probably represent the effect of ground anomalies. The next (second) row shows the intercept values for ΔH_0 (Dawn). The values are, in general, less negative as compared to ΔH_0 (Dusk) and lie in a range - 10 nT to - 31 nT. The general pattern is similar for both, indicating common ground anomaly effects, which are brought out clearly in the third row which shows the average for ΔH_0 (Dawn) and ΔH_0 (Dusk). Some striking features like the Bangui anomaly (0 to $+15^\circ$ longitude) are seen.

The fourth row shows the difference ΔH_0 (Dusk) minus ΔH_0 (Dawn). The values are consistently negative, in the range - 4 nT to - 20 nT with a standard error of about ± 4 nT. The difference could be interpreted as a quiet-time difference in Sq effect at Dawn and Dusk in the equatorial region. Sugiura and Hagan (1979) mention that, even at 0600 and 1800 LT, Sq exceeds 10 nT at southern midlatitudes. For the equatorial region, the X component in their Fig.2 shows negligible

ΔH at 0600 LT but considerable ΔH at 1800 LT (about 10 nT). Our results for ΔH are in rough agreement with their findings, as ΔH and ΔX are expected to show similar variations.

The other plots in Fig.10 refer to the Y and Z components. For ΔY_0 , values range from -11 nT to +27 nT for Dusk (fifth row) and -26 nT to +11 nT for Dawn (sixth row). Thus, positive as well as negative values are seen. Their average (seventh row) shows a range of only -11 nT to +17 nT. But the difference $\Delta Y_0(\text{Dusk})$ minus $\Delta Y_0(\text{Dawn})$ shown in the eighth row, has a very large range, viz. -11 nT to +29 nT. If interpreted as a difference in Sq effects at Dawn and Dusk, the effect in ΔY_0 is very large indeed, much larger than the effect in ΔH_0 , shown in the fourth row. The diagrams of Sugiura and Hagan (1979) do not indicate such large Sq differences in the ΔY component at equator. We suspect that a part of the ΔH_0 and ΔY_0 Dusk-Dawn differences seen in the fourth and the eighth row have some other origin than ionospheric Sq current effects.

The ninth and tenth row show $\Delta Z_0(\text{Dusk})$ and $\Delta Z_0(\text{Dawn})$. Here too, a considerable longitudinal variation is seen, from -22 nT to +17 nT for $\Delta Z_0(\text{Dusk})$ and -18 nT to +3 nT for $\Delta Z_0(\text{Dawn})$. Their average (eleventh row) has a range -19 nT to +10 nT while their difference (twelveth row) has a range -10 nT to +15 nT. Compared to ΔH_0 and ΔY_0 , the ΔZ_0 ranges are smaller but, by no means negligible. All these are, of course deviations from the model values and hence, show inadequacy of the model for representing the actual situation. What exactly the actual situation represents, (ground anomaly effects, differential Sq effects, some residual magnetospheric effects probably different for Dawn and Dusk) is a moot question.

In Fig.10, the values demonstrated refer to 5° intervals of longitude. This range was chosen on the rough assumption that, at MAGSAT altitudes (about 400 km), ground anomalies of roughly similar (or larger) dimensions would be effective. In particular cases, anomalies could be restricted to longitudes less than 5° in width

and these would be detectable if correlation analysis was carried out for narrower longitude intervals. However, in that case, the number of points (pairs) available for correlation would be rather small (presently, we had about 15) and the standard errors of the estimated values of the intercepts would increase. In Fig.10, the jump in values from one longitude interval to the next rarely exceeds 8 nT. (Actual values are given in Table 2). Thus an error of ± 4 nT is probably involved, which is only a little larger than the statistical standard error from the correlation analysis. Thus, the values plotted in Fig.10 and given in Table 2 should be considered as having errors of about ± 4 nT or less.

The values in Fig.10 are estimates of the ground anomaly effects as well as dusk-dawn difference of Sq effects at the geographic equator. However since the purpose of the present investigation is not to study either of these specifically but to examine storm-time variations, we propose to use these values only as base values or zero errors (ΔH_0 , ΔY_0 , ΔZ_0 for Dusk and Dawn separately) and propose to subtract these from the various passes at the appropriate longitudes for the appropriate parameters (ΔH_0 or ΔY_0 or ΔZ_0 , at Dusk or Dawn).

First, we examine how some parts of Fig.7 are affected when these base values are subtracted. Fig.11 (a) shows a plot of ΔH_0 (Dusk) versus ΔH_0 (Dawn) for Nov. 3-5, 1979, same as in Fig.7 (a). Whereas the points in Fig.11 (a) are nearer the origin (0,0) now, the scatter is quite large, indicating that, even after the base-value corrections (which are different for different longitudes as given in Table 2) are applied, the ΔH_0 (Dawn) and ΔH_0 (Dusk) values do not show parallel variations. In Fig.11 (b) we show the plot for the first major storm viz. Nov. 11-15, 1979, same as in Fig.7 (c). Here, a spectacular hysteresis loop is noticed. Thus, in the main phase of the storm (Nov. 11-13), ΔH_0 (Dusk) seems to attain negative values numerically almost double of those of ΔH_0 (Dawn). Somewhere near the end of the main phase, ΔH_0 (Dusk) saturates. The ΔH_0 (Dawn) continues to increase (negatively) but never

catches up with $\Delta H_0(\text{Dusk})$. Only during the recovery of $\Delta H_0(\text{Dusk})$, both $\Delta H_0(\text{Dusk})$ and $\Delta H_0(\text{Dawn})$ become almost equal and reach zero level together. In Fig.7 (c) too (for the uncorrected values) such a hysteresis pattern was discernible.

In the period under consideration, (Nov. 2, 1979 to Jan. 18, 1980), there was one more major storm viz. Dec.31, 1979 - Jan. 3, 1980. After correcting for base values, Fig. 11 (c) shows the plot for $\Delta H_0(\text{Dusk})$ versus $\Delta H_0(\text{Dawn})$, for this storm. The hysteresis loop is evident and $\Delta H_0(\text{Dawn})$ never reaches the highest level of $\Delta H_0(\text{Dusk})$.

Fig.12 shows a sequential plot of $\Delta H_0(\text{Dusk})$ and $\Delta H_0(\text{Dawn})$ for the storm of Nov. 11-15, 1979. The top curves (first row) are for $\Delta H_0(\text{Dawn})$ (full lines) and $\Delta H_0(\text{Dusk})$ (dashes and crosses) and are the same as in Fig.1. The next plot (second row) is for Dst, also same as in Fig.1. The third and fourth row plots are for the Y and Z components respectively. The idea was to check whether these components also exhibited some storm effects. The $\Delta Y_0(\text{Dawn})$ and $\Delta Y_0(\text{Dusk})$ seem to show considerable divergence during the main phase (Nov. 13), indicating that the ring current plane was not coincident with the earth's geographical equatorial plane. A slight angle is indicated, so that Dusk and Dawn sides show reverse patterns. For the Z component too, some differences in $\Delta Z_0(\text{Dawn})$ and $\Delta Z_0(\text{Dusk})$ are indicated, though the magnitude is smaller than ΔY_0 differences.

All these values are yet uncorrected for the base values given in Table 2. The fifth, sixth and seventh rows in Fig.12 show the corrected values of ΔH_0 , ΔY_0 and ΔZ_0 for Dawn (full lines) and Dusk (dashes and crosses). The $\Delta H_0(\text{Dusk})$ and $\Delta H_0(\text{Dawn})$ now are very similar to each other during quiet periods (Nov. 11,12), indicating that the dissimilarities in the top plot (first row) were mainly due to large and variable zero errors. For the main phase (Nov. 13), $\Delta H_0(\text{Dusk})$ is almost double of $\Delta H_0(\text{Dawn})$ and, only when $\Delta H_0(\text{Dusk})$ starts recovering on Nov. 14, $\Delta H_0(\text{Dawn})$ catches up with $\Delta H_0(\text{Dusk})$ and, the two have a similar recovery thereafter. For ΔY_0 (sixth row),

the values for both Dusk and Dawn are almost zero for quiet periods. But, during the peak of the main phase (late Nov. 13 and early Nov. 14), ΔY_0 (Dusk) is vastly different from ΔY_0 (Dawn), by several tens of nT. Thus, there is an indication of some meridional component, which could also be due to nonparallelism between the central plane of the ring current and the geographical equatorial plane.

The seventh row shows ΔZ_0 variation. As compared to the fourth row, the variations in the seventh row are reduced. However, a slight storm effect with ΔZ_0 (Dusk) and ΔZ_0 (Dawn) differing by about 20 nT is seen on Nov. 13-14.

Fig.13 shows the corrected values of ΔH_0 , ΔY_0 and ΔZ_0 for the other major storm viz. of Dec. 31, 1979 to Jan. 2, 1980. For ΔH_0 , the ΔH_0 (Dawn) seems to be less affected, so much so that the minor storm at the end part of Dec. 31, as seen in Dst (about - 40 nT) is not seen for ΔH_0 (Dawn) but is seen for ΔH_0 (Dusk). In the main storm too (latter half of Jan. 1), ΔH_0 (Dawn) showed storm-effects later and smaller in magnitude as compared to ΔH_0 (Dusk). The hysteresis loop is already shown in Fig.11(c).

For ΔY_0 , there is a considerable difference between ΔY_0 (Dusk) and ΔY_0 (Dawn) both in the end part of Dec. 31 and the end part of Jan. 1. Thus, at the peak of the main phase, considerable Dawn-Dusk asymmetries even in the ΔY component were seen. For ΔZ_0 , the effect is smaller but noticeable in the end part of Jan. 1.

From Figs 12 and 13, it seems that the orientation of the ring current vis a vis the geographical equator is different in the Dawn and Dusk sectors.

Since an important purpose of the present investigation was to compare storm-effects at ground and at MAGSAT altitudes, we obtained from WDC-A, Boulder the hourly values of the H component for several low and mid-latitude locations, as listed in Table 3 according to geographical longitudes. Some of these could be

considered as in the same longitude belt. For example, Tsumeb, Bangui and Hermanus have roughly the same longitude (about 15°E). For these locations, there would be one Dawn pass and one Dusk pass per day which could be compared with ground ΔH values at Dawn and Dusk, choosing the proper geographical latitudes on the passes to match with the geographical latitudes of the ground stations as given in Table 3. Since hourly values (near Dusk or Dawn) are used, there is a possible error of half an hour in time. Also, a pass may not occur exactly at a given ground location longitude but there will generally be a pass within about $\pm 10^{\circ}$ of the longitude of the location. Thus, inaccuracies of about 1/2 hour in time and about 10° in space are involved. Fortunately, in quiet periods, the successive hourly values at Dawn and Dusk do not change by more than a few nT nor do the ΔH values in successive passes. During disturbed periods, errors of ± 5 nT could occur on these counts.

For the month of November 1979, we omitted data for Nov. 2, 1979 as these seemed doubtful for the satellite data. For the 28 days Nov. 3-30, Fig. 14 shows a plot of ΔH at ground for Bangui (4.6°N , 18.6°E) versus ΔH at MAGSAT for passes near 18.6°E (within $\pm 10^{\circ}$) for Dawn passes in the left half and Dusk passes in the right half, with 28 pairs of values in each graph. For ground values, the base is arbitrary. Also for satellite values, no base-value corrections are applied as, for this given longitude, the same base value would be applicable to all values. The purpose of this plot is not to estimate the intercepts on the axes (as was done in Figs 8 and 9) but to estimate the slope values. For this, a correlation analysis was carried out between the 28 pair of values of ΔH at satellite (for geographical latitude 5°N , appropriate for Bangui) for Nov. 3-30, 1979. The correlation coefficient was high (exceeding + 0.9) and the two regression lines ($Y = mX + c$) one with ground ΔH as the independent variable Y and the ΔH at satellite as the dependent variable X (and the other, vice versa) were very close to each other, for both the Dusk passes and Dawn passes, as can be seen in Fig.14. The values of the correlation coefficients and the slope m(with standard errors) are given in Table 3, for Bangui as also for all the other locations.

All the correlations in Table 3 are high (exceeding +0.8). Also, within the standard errors of about 10%, all slopes are near unity. Since the period Nov. 3-30, 1979 had one major storm (Nov. 11-15) and a few minor storms, we conclude that, within an error of about 10%, which may very well be due to time and position inaccuracies inherent in this analysis, the ΔH effects at ground and at satellite (MAGSAT) altitudes have turned out to be identical. Thus, most of these effects are of magnetospheric origin and ionospheric effects, if any, are less than 10%, for the Dawn and Dusk periods.

At the bottom of Table 3, we give the average values of the slopes, which are slightly higher for Dusk and also when satellite ΔH is the independent variable Y . Thus, effects at satellite are probably ~3% higher than at ground.

4. Summary of the significant results

The results of the present analysis can be summarised as follows:

- (i) ΔH_0 (Dawn) and ΔH_0 (Dusk), are defined as the deviations of the observed values from the model values, for the H component at geographic equator, normalised to a constant geocentric distance of 6800 km. In general, these values were negative and, unequal for Dawn and Dusk. About 1200 Dawn passes and 1200 Dusk passes for the 78 days interval Nov. 2, 1979 to Jan. 18, 1980 were separated into 5° longitude groups as, -180° to -175° , -175° to -170° , -5° to 0° , 0° to $+5^\circ$ $+175^\circ$ to $+180^\circ$. In each group, there were roughly 15 passes and for these, Dst was plotted versus ΔH_0 (Dawn) and ΔH_0 (Dusk). A high correlation was obtained. From the regression analysis, ΔH_0 (Dawn) and ΔH_0 (Dusk) i.e. the intercepts on the ΔH_0 axis, were obtained. These are the base values of ΔH_0 (Dawn) and ΔH_0 (Dusk) for quiet periods (Dst = 0).

These intercepts were obtained for the other components also (ΔY_0 and ΔZ_0) and are given in Table 3, with standard errors.

(ii) From the observed values of ΔH_0 (Dawn) and ΔH_0 (Dusk), the base values for the appropriate longitude groups were subtracted. The residual ΔH_0 (Dawn) and ΔH_0 (Dusk) were studied for storm-time variations. For the two major storms of Nov. 11-15, 1979 and Dec. 31, 1979 - Jan. 2, 1980, the following was observed:

- (a) During quiet periods, both ΔH_0 (Dawn) and ΔH_0 (Dusk) were almost zero.
- (b) When a storm commenced, as seen by Dst attaining large negative values, the ΔH_0 (Dusk) responded first and attained values similar to Dst. The ΔH_0 (Dawn) did not respond to small Dst changes. For large Dst (negative), ΔH_0 (Dusk) followed suit but ΔH_0 (Dawn) lagged behind and never reached ΔH_0 (Dusk) or Dst levels. After Dst and ΔH_0 (Dusk) started recovery, ΔH_0 (Dawn) caught up with the same and thereafter, all the three recovered together. A plot of ΔH_0 (Dusk) versus ΔH_0 (Dawn) showed hysteresis loops, for both the storms.

It seems that the storm-effects are more intense and are seen earlier in the Dusk sector, as compared to the Dawn sector.

- (c) During storm main phase, ΔY_0 (Dawn) and ΔY_0 (Dusk) show large variations. Thus, some meridional currents are indicated. These could be due to the plane of the ring current not coinciding with the geographic equatorial plane. Small effects in ΔZ_0 are also seen.
- (iii) A comparison of ΔH at ground near Dawn and Dusk and ΔH values at MAGSAT altitudes, for the latitude and longitude appropriate for the ground location showed high correlations

and a slope of almost unity. Thus, variations at ground and at MAGSAT altitudes were found to be identical, within a standard error of $\pm 10\%$. Thus, both these seem to be mostly of magnetospheric origin; and, ionospheric effects, if any, are less than $\pm 10\%$, for the Dawn and Dusk periods. This does not exclude the possibility of ionospheric effects at other local times.

- (iv) For the base-level values given in Table 3 for $\Delta\bar{H}_0$, $\Delta\bar{V}_0$, $\Delta\bar{Z}_0$, possible explanations are (a) Ground anomaly effects and (b) Sq effects. However, it is quite likely that some quiet-time magnetospheric effects are also involved.

5. Data Quality

As mentioned in the earlier report, the latitude distribution of ΔH in some passes seemed to be very odd. As a quantitative measure of this distribution, we calculated the standard deviation (σ) for each pass.

For about 1200 Dawn passes and about 1200 Dusk passes, Fig. 15 shows the frequency distribution for σ (nT). As can be seen, a vast majority of passes have σ between 0 and 10 nT, the peaks occurring at 5 nT for the Dusk passes and 3 nT for the Dawn passes. For some passes, σ exceeds 10 nT and for a few σ is abnormally high. We consider these as faulty passes. Table 4 gives the frequency distribution and Table 5 enlists the faulty Pass numbers, separately for Dawn and Dusk. In Fig. 16, the latitudinal plots for some passes are illustrated. In Fig. 16 (a), we show passes with σ less than 10 nT. Here, passes are chosen with different levels of ΔH . Thus, passes at the top have very low ΔH and are quiet day passes (Pass numbers are indicated). Passes at the bottom have ΔH as large as - 150 and these are storm-time passes. But all these show a small latitude variation ($\sigma < 10$ nT) and we consider these as good, acceptable passes. As can be seen from Table 4, about 96% of the Dawn passes and

92% of the Dusk passes are good passes by this criterion. In Fig.16 (b) we plot the latitudinal distribution of some passes with σ between 10 nT and 30 nT. The latitude distribution is odd and erratic. Note that the vertical scale in Fig.16 (b) is compressed by a factor of 2 as compared to Fig.16 (a). In Fig.16 (c), we show passes which are extremely erratic. The vertical scale is highly compressed. The values of σ exceed 50 nT. We consider it undesirable to use these passes for any analysis. In Table 5, the Passes in the top part are the most unreliable, with faultiness lesser and acceptability more for lower rows in Table 5.

It would be of interest to know whether other MAGSAT workers have identified these passes as faulty.

In the present analysis, we have used the X, Y, Z components in NEV coordinates and the corresponding XMD, YMD, ZMD. For a part of the analysis, we used XA, YA, ZA also, which are the averages of X, Y, Z for the 80 CHRONICLE input points. The results for XA, YA, ZA tallied with those for X, Y, Z within ± 2 nT. For passes for which σ was abnormally large (bad passes), the fault was seen in XA, YA, ZA also.

6. Future plans

The major part of the present investigation is over. In future, we propose to examine the latitude dependence of storm effects.

REFERENCES

Sugiura M. and Hagan M.P. Geomagnetic Sq variation at satellite altitudes: Is Sq correction important in MAGSAT data analysis? Geophys. Res. Letters 6, 397-400(1979).

CAPTIONS FOR FIGURES

Fig. 1 - Plots of ΔH_0 i.e. the deviations $\Delta H = H(\text{Observed})$ minus $H(\text{Model})$ for equatorial crossings (normalised to a geocentric distance of 6800 km), for Dusk (crosses and dashes) and Dawn (dots and full lines), as also of Dst, for Nov. 2-19, 1979. Kp is also indicated as histograms.

Fig. 2 - Plots of ΔH_0 etc. for Nov. 20 - Dec. 1, 1979.

Fig. 3 - Plots of ΔH_0 etc. for Dec. 2-13, 1979.

Fig. 4 - Plots of ΔH_0 etc. for Dec. 14-25, 1979.

Fig. 5 - Plots of ΔH_0 etc. for Dec. 26, 1979 - Jan. 6, 1980.

Fig. 6 - Plots of ΔH_0 etc. for Jan. 7-18, 1980.

Fig. 7 - ΔH_0 (Dusk) versus ΔH_0 (Dawn) for
(a) Nov. 3-5, 1979
(b) Nov. 7-10, 1979 (crosses show doubtful Dusk values)
(c) Nov. 11-15, 1979 (storm period, crosses represent Recovery, Nov. 14, 15)
(d) Nov. 16-20, 1979
Regression lines and correlation coefficients γ are indicated.

Fig. 8 - Dst versus ΔH_0 (Dawn) (left half) and ΔH_0 (Dusk) (right half) for the 5° longitude belts (a) Longitude 0° to $+5^\circ$ and (b) Longitude $+5^\circ$ to $+10^\circ$. The correlation coefficients γ and the regression lines are indicated. Circled numbers indicate intercepts on the ΔH_0 axis and represent the base values for ΔH_0 (Dawn) and ΔH_0 (Dusk) for the two longitude groups.

Fig. 9 - Same as Fig. 8 but for longitude groups (a) $+10^\circ$ to $+15^\circ$ and (b) $+15^\circ$ to $+20^\circ$.

Fig. 10 - Longitudinal distribution of the base values $\Delta\overline{H}_0$, $\Delta\overline{Y}_0$, $\Delta\overline{Z}_0$ for Dawn and Dusk, the average (AVER) for Dusk and Dawn and the difference (DIFF) between Dusk and Dawn. Negative values are shown shaded.

Fig. 11 - ΔH_0 (Dusk) versus ΔH_0 (Dawn) using values corrected for base levels.

(a) Nov. 3-5, 1979

(b) Nov. 11-15, 1979 (Storm period, crosses refer to Recovery, Nov. 14, 15)

(c) Dec. 31, 1979 - Jan. 3, 1980 (Storm period, crosses refer to Recovery, Jan. 2, 3).

Fig. 12 - Plots for the storm period Nov. 11-15, 1979 for Dawn (dots and full lines) and Dusk (dashes and crosses).

Row 1:- ΔH_0 (Dusk) and ΔH_0 (Dawn) uncorrected

Row 2:- Dst

Row 3:- ΔY_0 (Dusk) and ΔY_0 (Dawn) uncorrected

Row 4:- ΔZ_0 (Dusk) and ΔZ_0 (Dawn) uncorrected

Rows 5, 6, 7:- ΔH_0 , ΔY_0 , ΔZ_0 , corrected for base values.

Fig. 13 - Plots of Dst and the base-level-corrected values of ΔH_0 , ΔY_0 , ΔZ_0 for Dawn (dots with full lines) and Dusk (dashes with crosses), for the storm period Dec. 31, 1979 - Jan. 2, 1980.

Fig. 14 - ΔH at Bangui (5°N , 19°E) versus MAGSAT ΔH_0 values at 5°N for Dawn and Dusk passes near 19°E longitude, for Nov. 3-30, 1979. Excellent correlation with regression lines of slope almost unity are indicated, implying very good parallelism between ground variations and MAGSAT variations.

Fig. 15 - Frequency distribution of the Standard Deviation (σ) for about 1200 Dusk passes (upper half) and Dawn passes (lower half). Pass numbers for abnormally large σ are indicated.

Fig. 16 - The latitudinal distribution of ΔH for a few selected passes with

(a) σ less than 10 nT

(b) σ less between 10 nT and 30 nT

(c) σ exceeding 50 nT.

Labels indicate Pass number and LT (Dusk or Dawn).

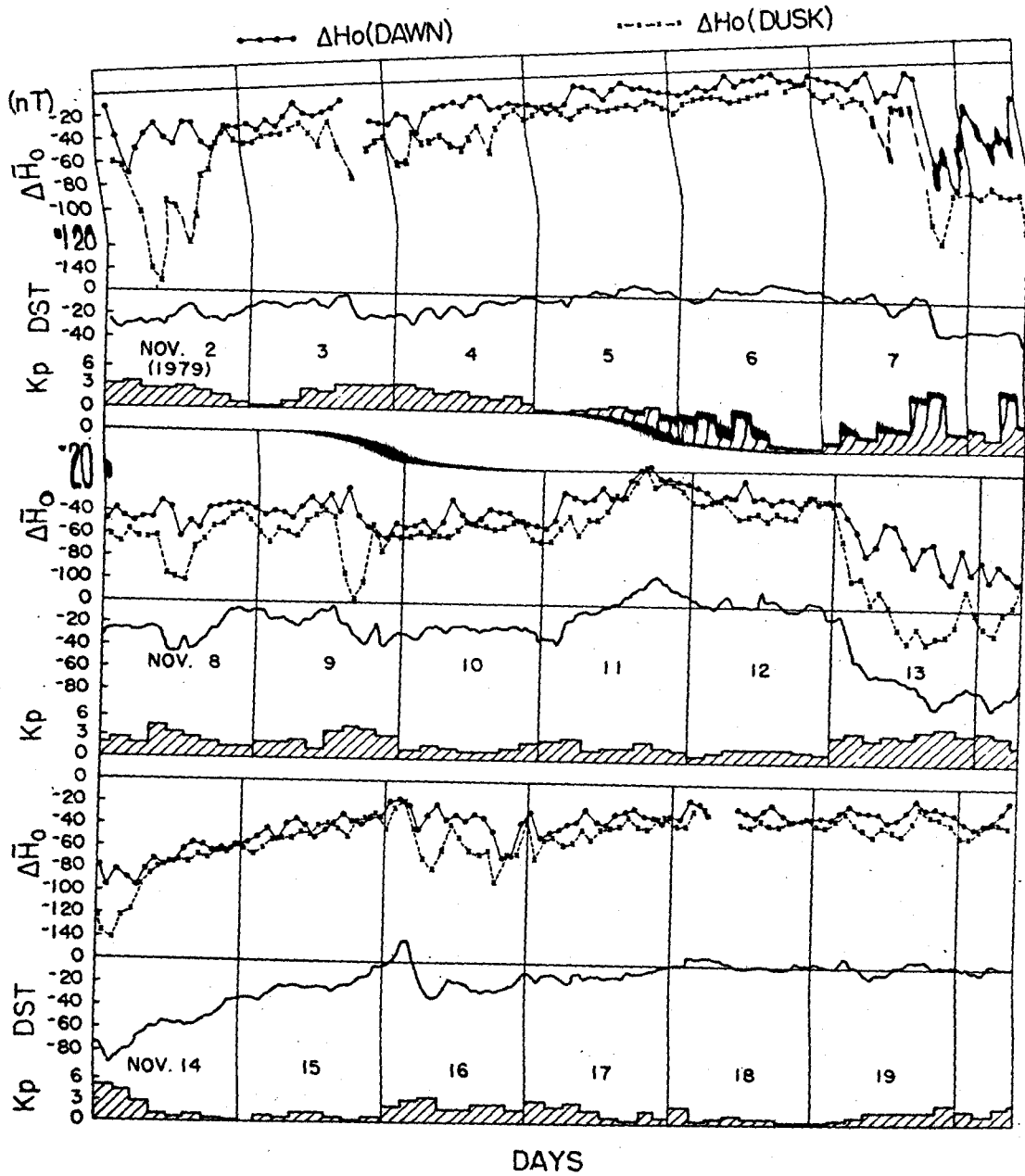


Fig. 1 - Plots of ΔH_0 i.e. the deviations $\Delta H = H(\text{Observed})$ minus $H(\text{Model})$ for equatorial crossings (normalised to a geocentric distance of 6800 km), for Dusk (crosses and dashes) and Dawn (dots and full lines), as also of Dst, for Nov. 2-19, 1979. Kp is also indicated as histograms.

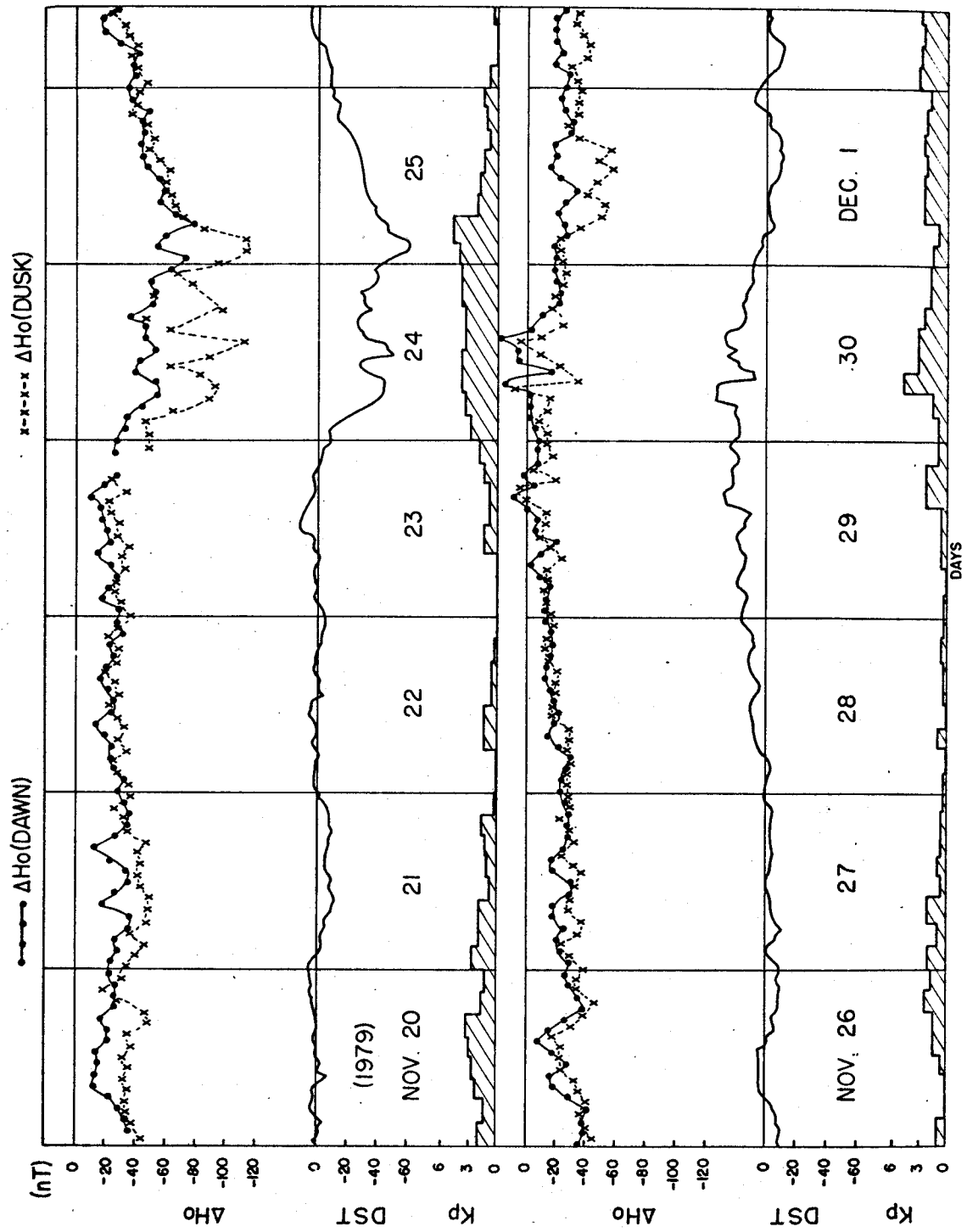


Fig. 2 - Plots of ΔH_0 etc. for Nov. 20 - Dec. 1, 1979.

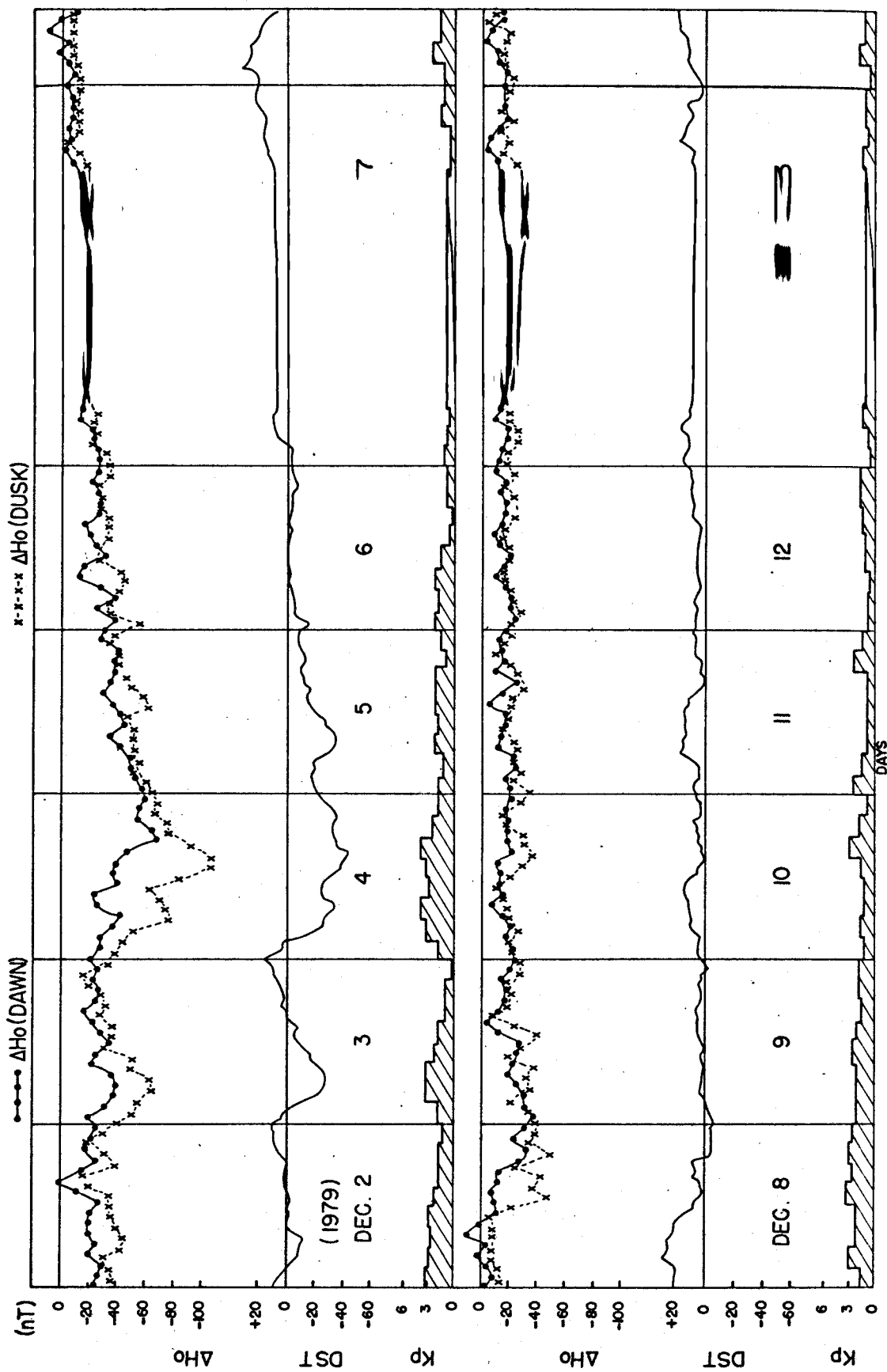


Fig. 3 - Plots of ΔH_0 etc. for Dec. 2-13, 1979.

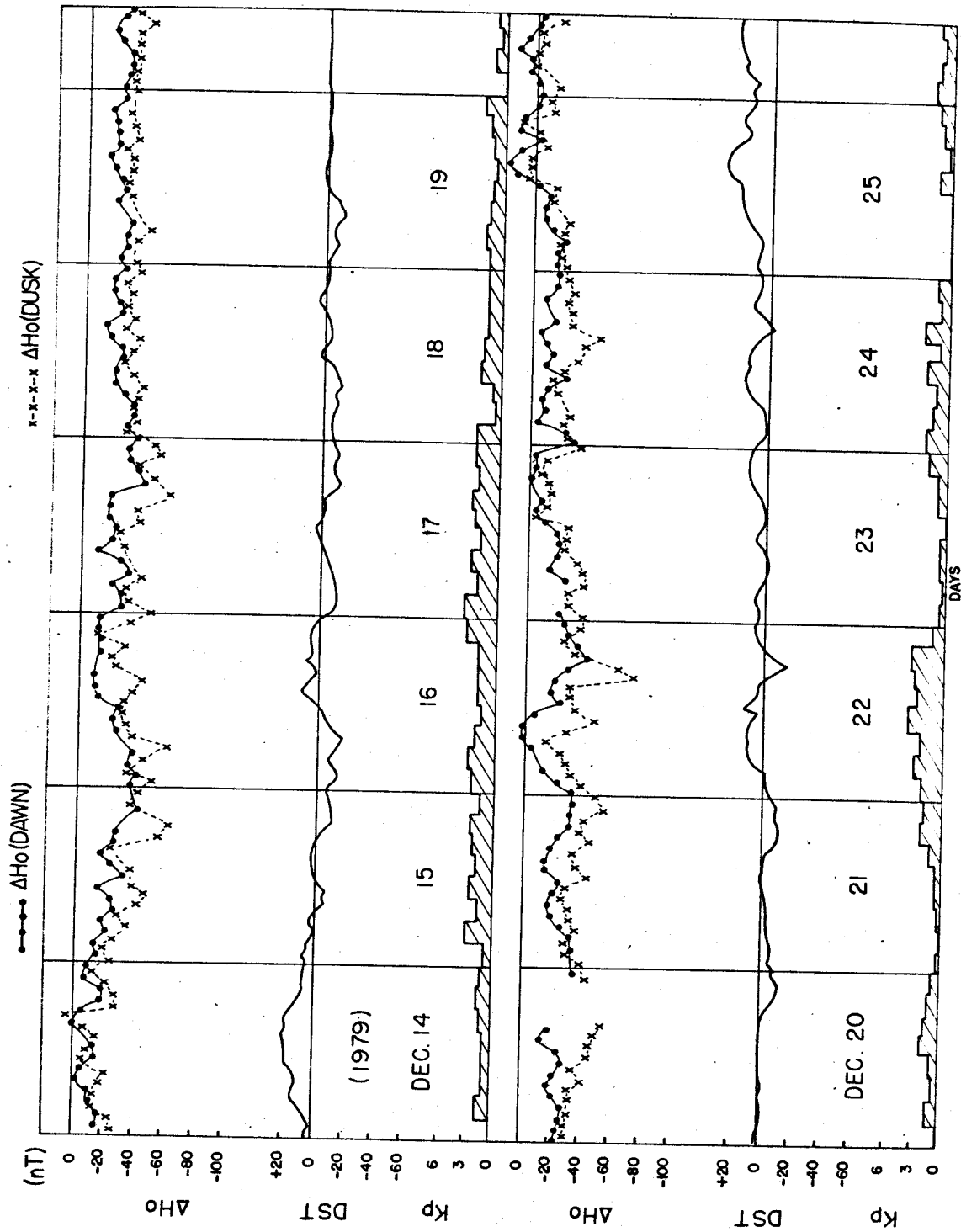


Fig. 4 - Plots of ΔH_0 etc. for Dec. 14-25, 1979.

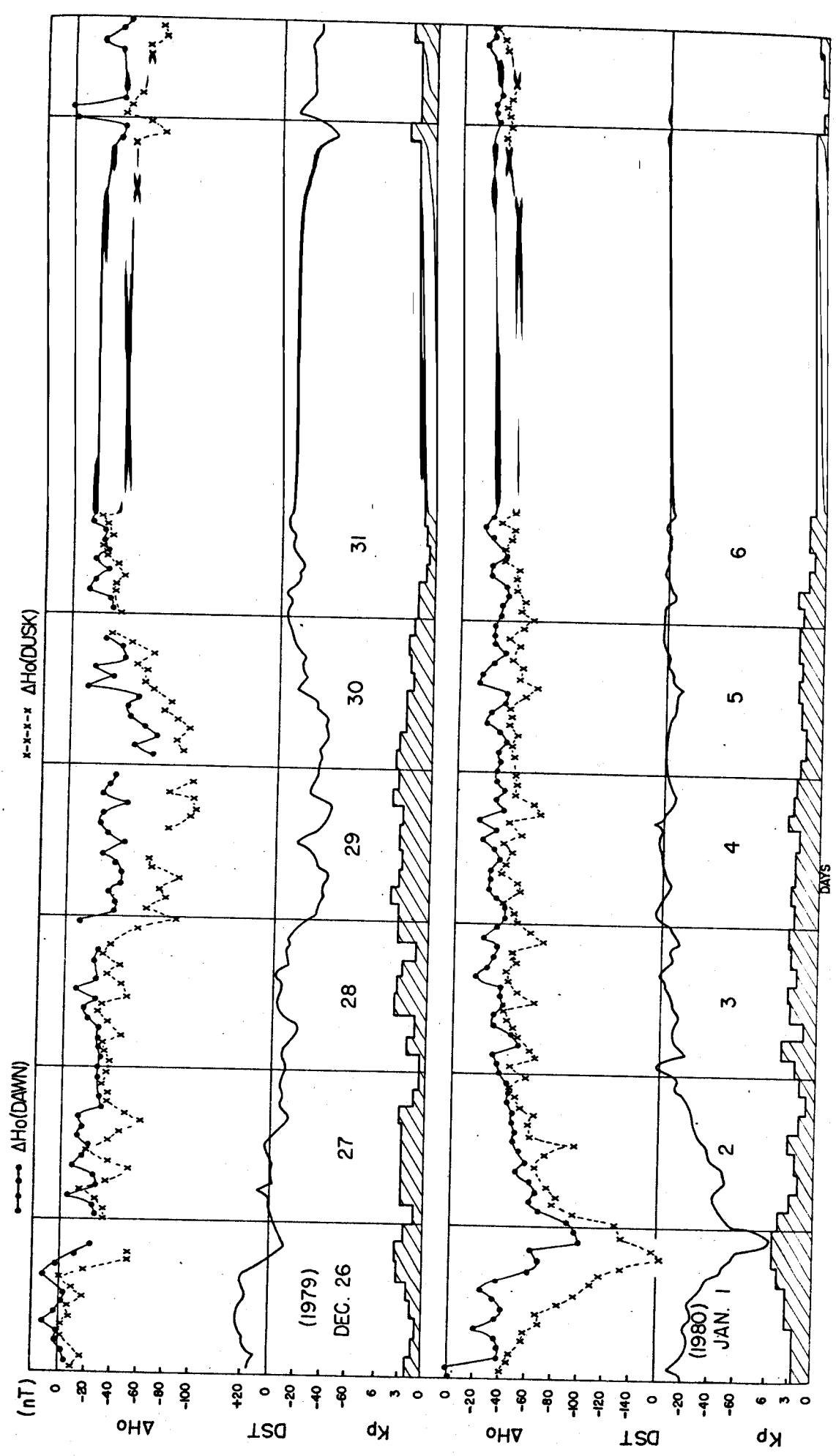


Fig. 5 - Plots of ΔH_0 etc. for Dec. 26, 1979 - Jan. 6, 1980.

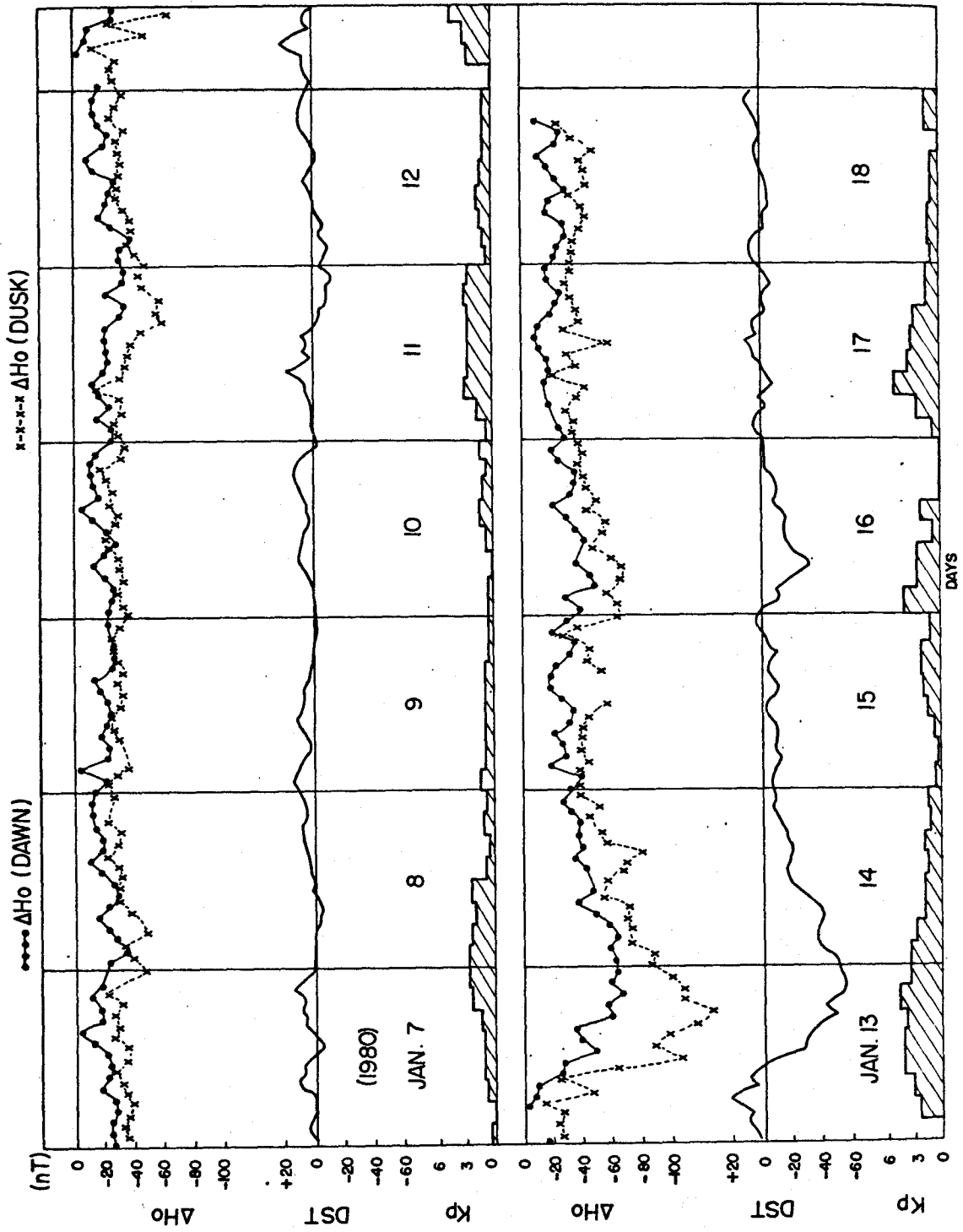


Fig. 6 - Plots of ΔH_0 etc. for Jan. 7-18, 1980.

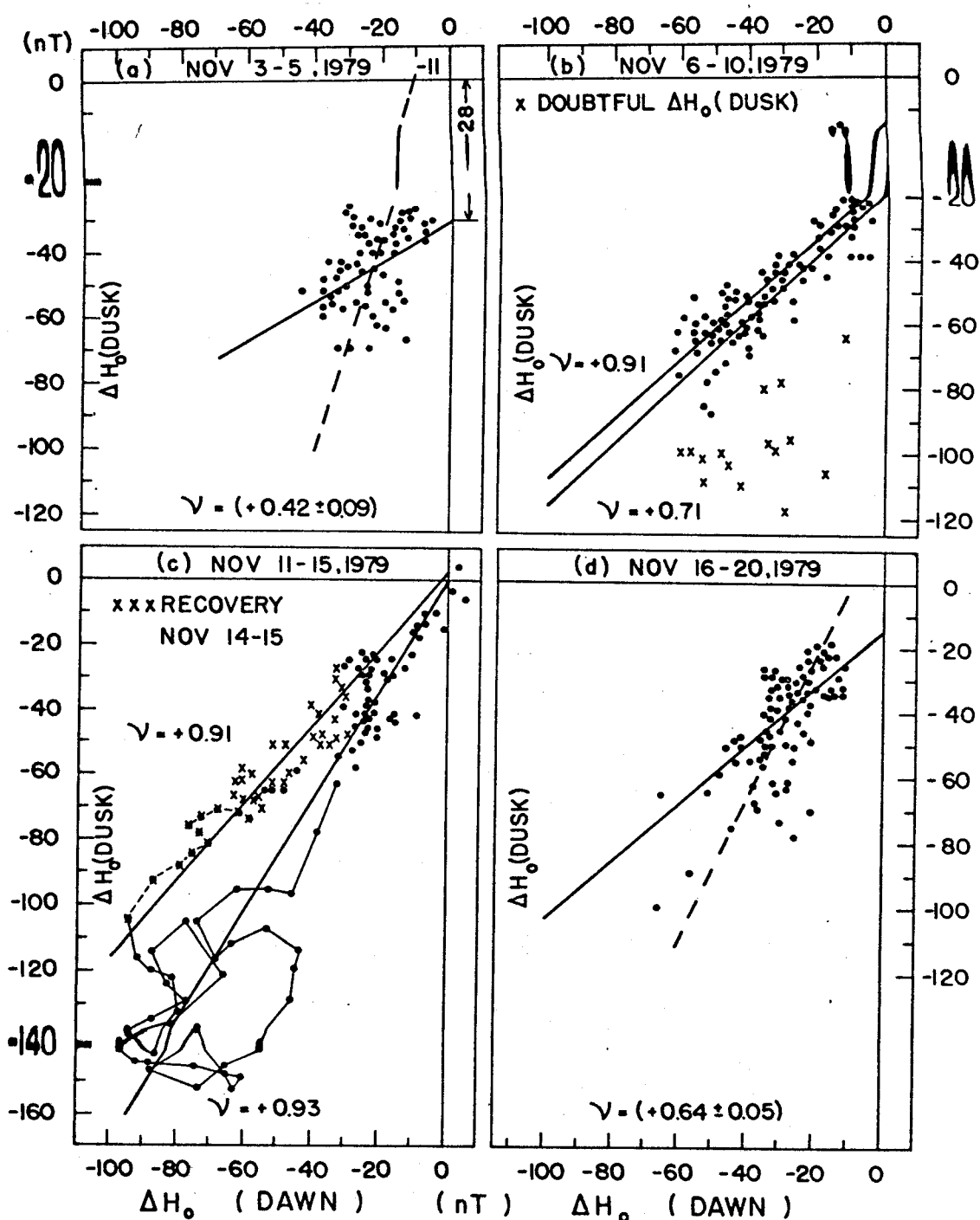


Fig. 7 - ΔH_0 (Dusk) versus ΔH_0 (Dawn) for
 (a) Nov. 3-5, 1979
 (b) Nov. 7-10, 1979 (crosses show doubtful Dusk values)
 (c) Nov. 11-15, 1979 (storm period, crosses represent Recovery, Nov. 14, 15)
 (d) Nov. 16-20, 1979
 Regression lines and correlation coefficients γ are indicated.

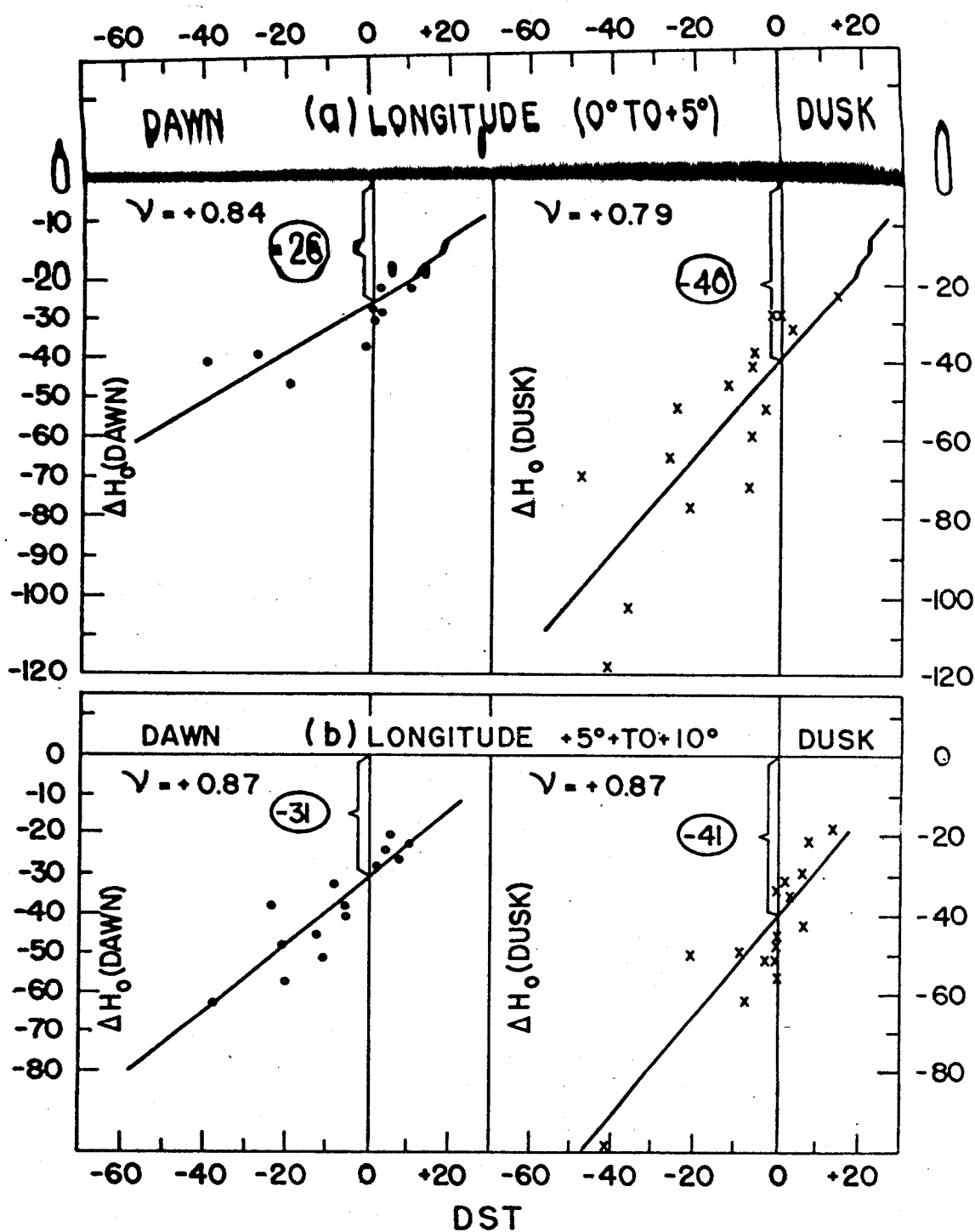


Fig. 8 - Dst versus ΔH_0 (Dawn) (left half) and ΔH_0 (Dusk) (right half) for the 5° longitude belts (a) Longitude 0° to $+5^\circ$ and (b) Longitude $+5^\circ$ to $+10^\circ$. The correlation coefficients γ and the regression lines are indicated. Circled numbers indicate intercepts on the ΔH_0 axis and represent the base values for ΔH_0 (Dawn) and ΔH_0 (Dusk) for the two longitude groups.

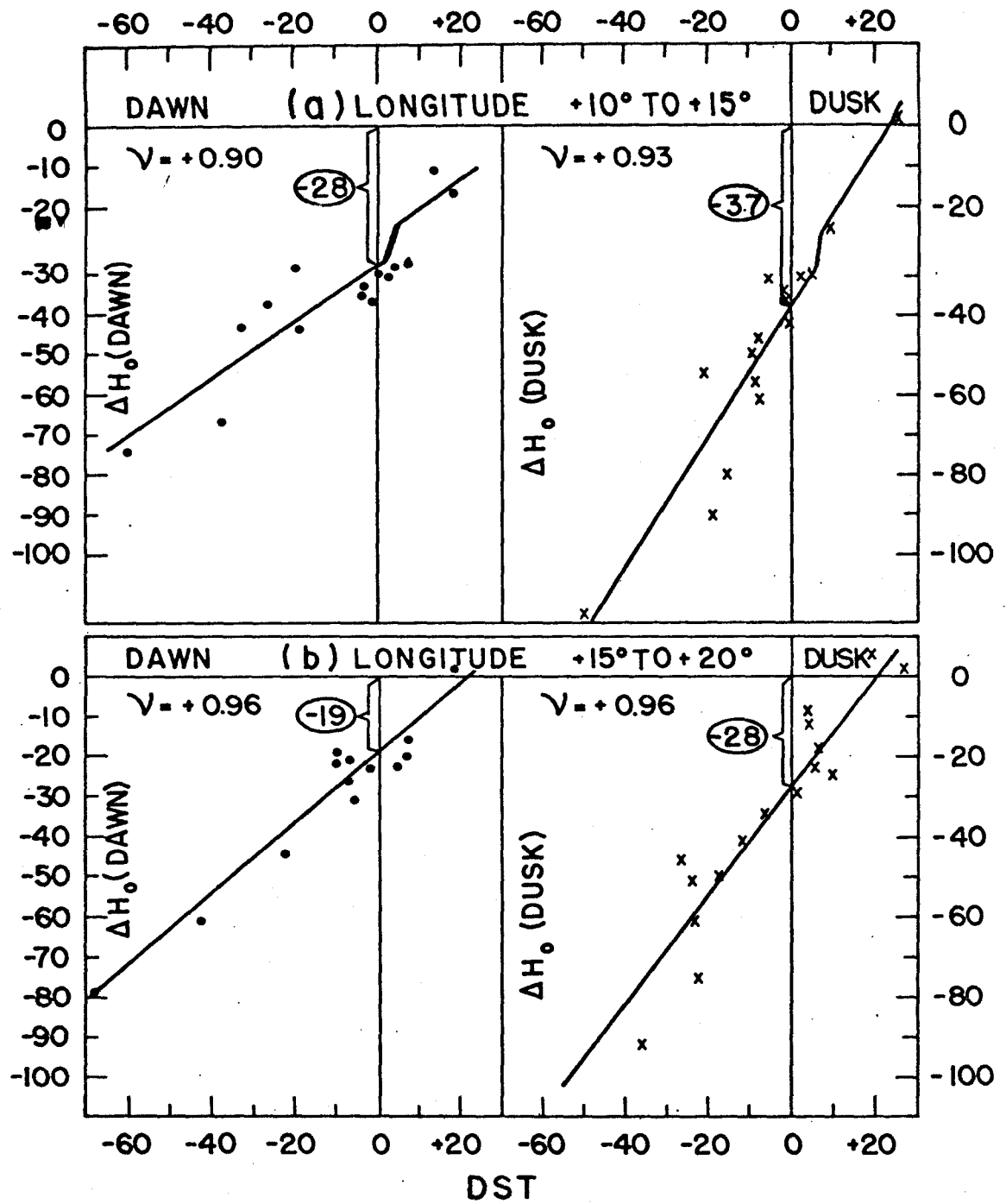


Fig. 9 - Same as Fig. 8 but for longitude groups (a) $+10^\circ$ to $+15^\circ$ and (b) $+15^\circ$ to $+20^\circ$.

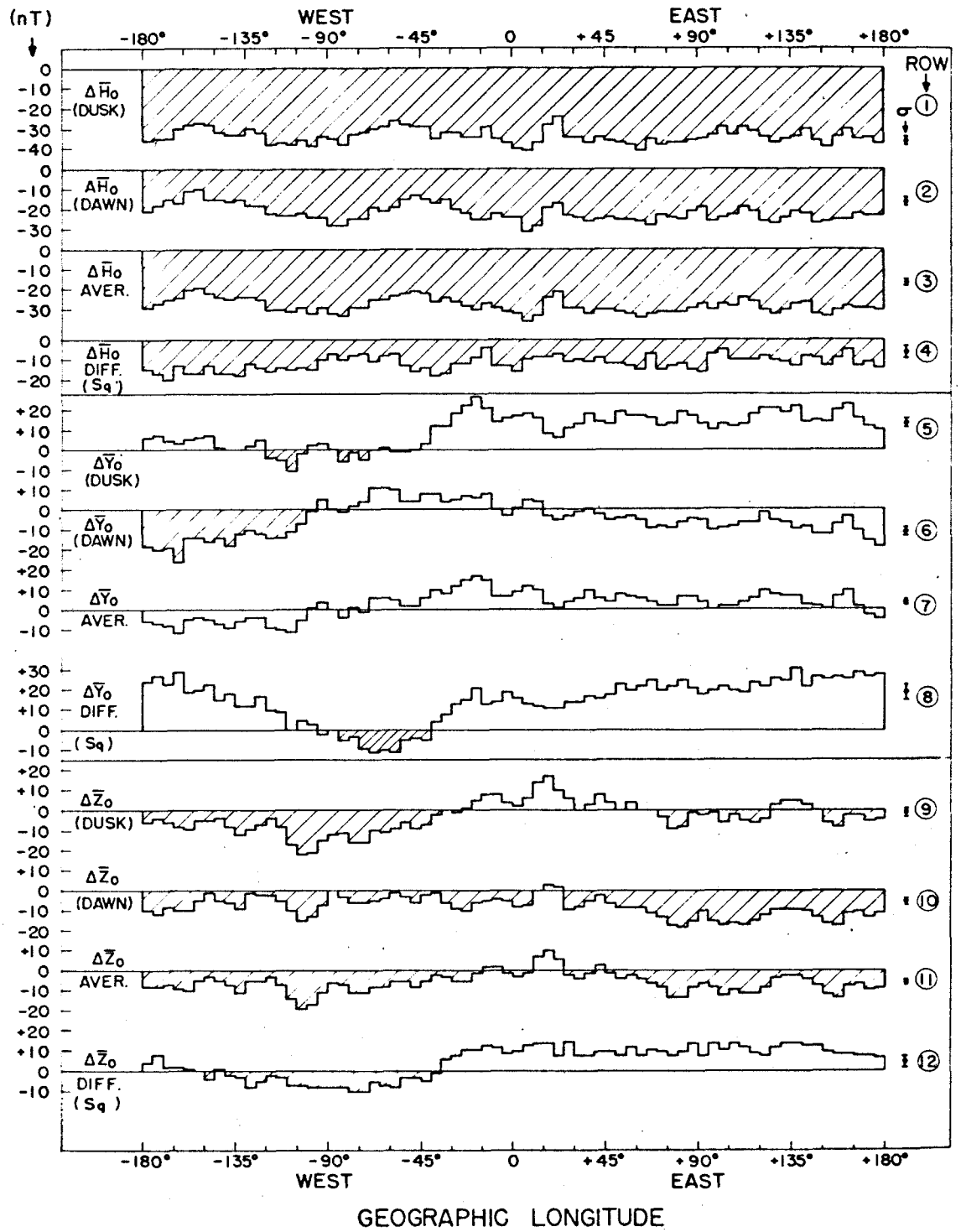


Fig. 10 - Longitudinal distribution of the base values $\Delta \bar{H}_0$, $\Delta \bar{Y}_0$, $\Delta \bar{Z}_0$ for Dawn and Dusk, the average (AVER) for Dusk and Dawn and the difference (DIFF) between Dusk and Dawn. Negative values are shown shaded.

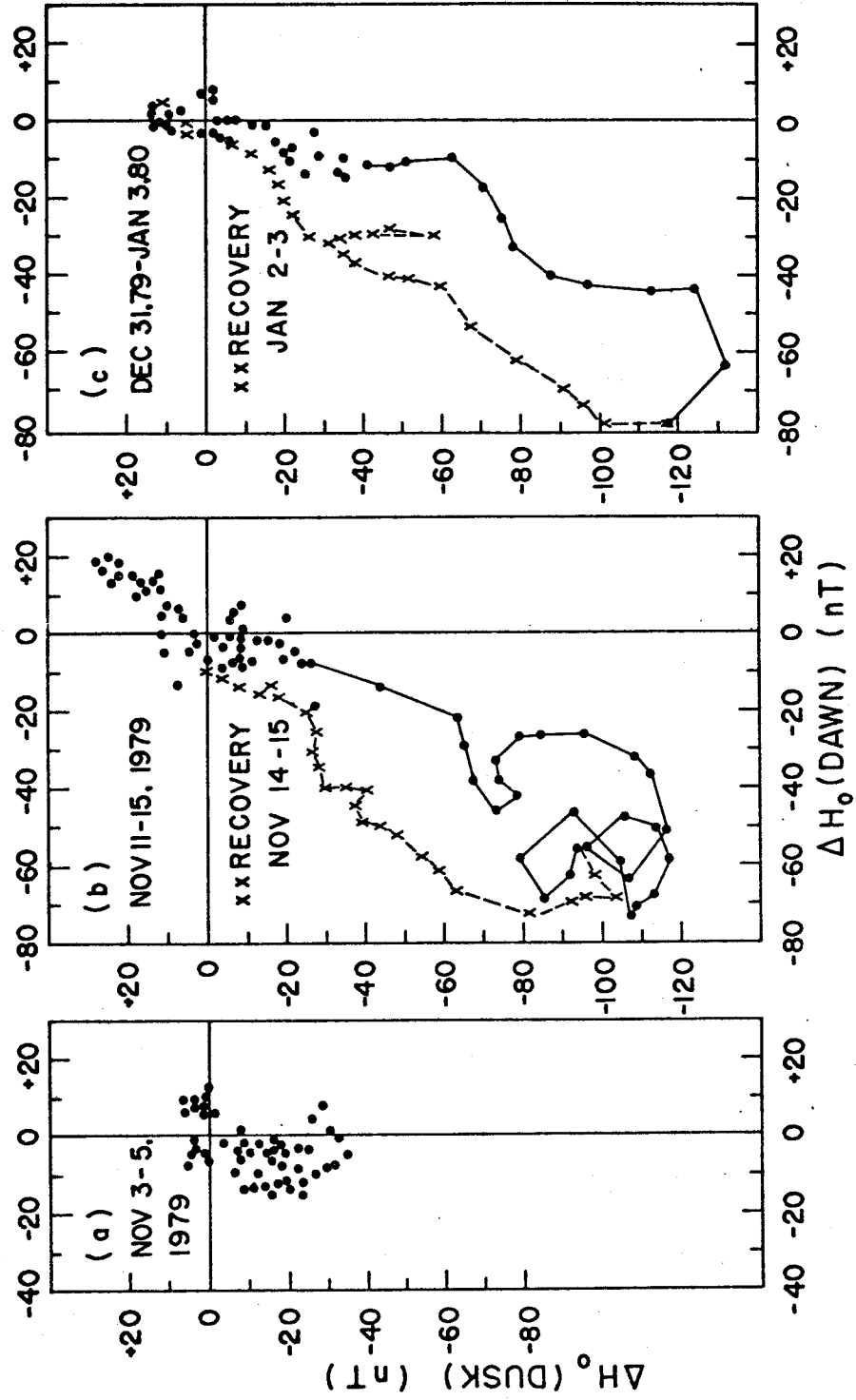


Fig. 11 - ΔH_0 (Dusk) versus ΔH_0 (Dawn) using values corrected for base levels.
 (a) Nov. 3-5, 1979
 (b) Nov. 11-15, 1979 (Storm period, crosses refer to Recovery, Nov. 14, 15)
 (c) Dec. 31, 1979 - Jan. 3, 1980 (Storm period, crosses refer to Recovery, Jan. 2, 3).

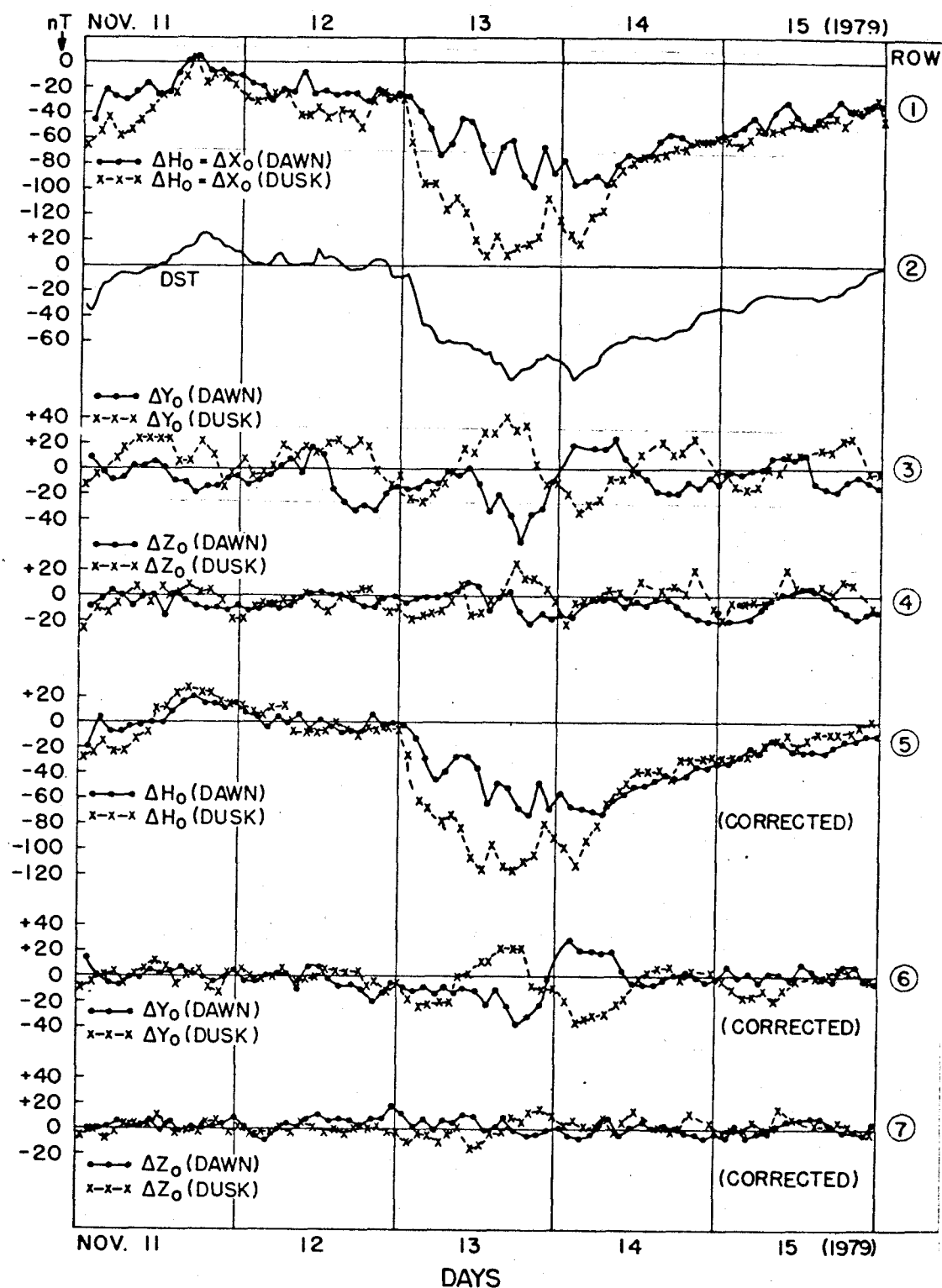


Fig. 12 - Plots for the storm period Nov. 11-15, 1979 for Dawn (dots and full lines) and Dusk (dashes and crosses).
 Row 1:- ΔH_0 (Dusk) and ΔH_0 (Dawn) uncorrected
 Row 2:- Dst
 Row 3:- ΔY_0 (Dusk) and ΔY_0 (Dawn) uncorrected
 Row 4:- ΔZ_0 (Dusk) and ΔZ_0 (Dawn) uncorrected
 Rows 5, 6, 7:- ΔH_0 , ΔY_0 , ΔZ_0 corrected for base values.

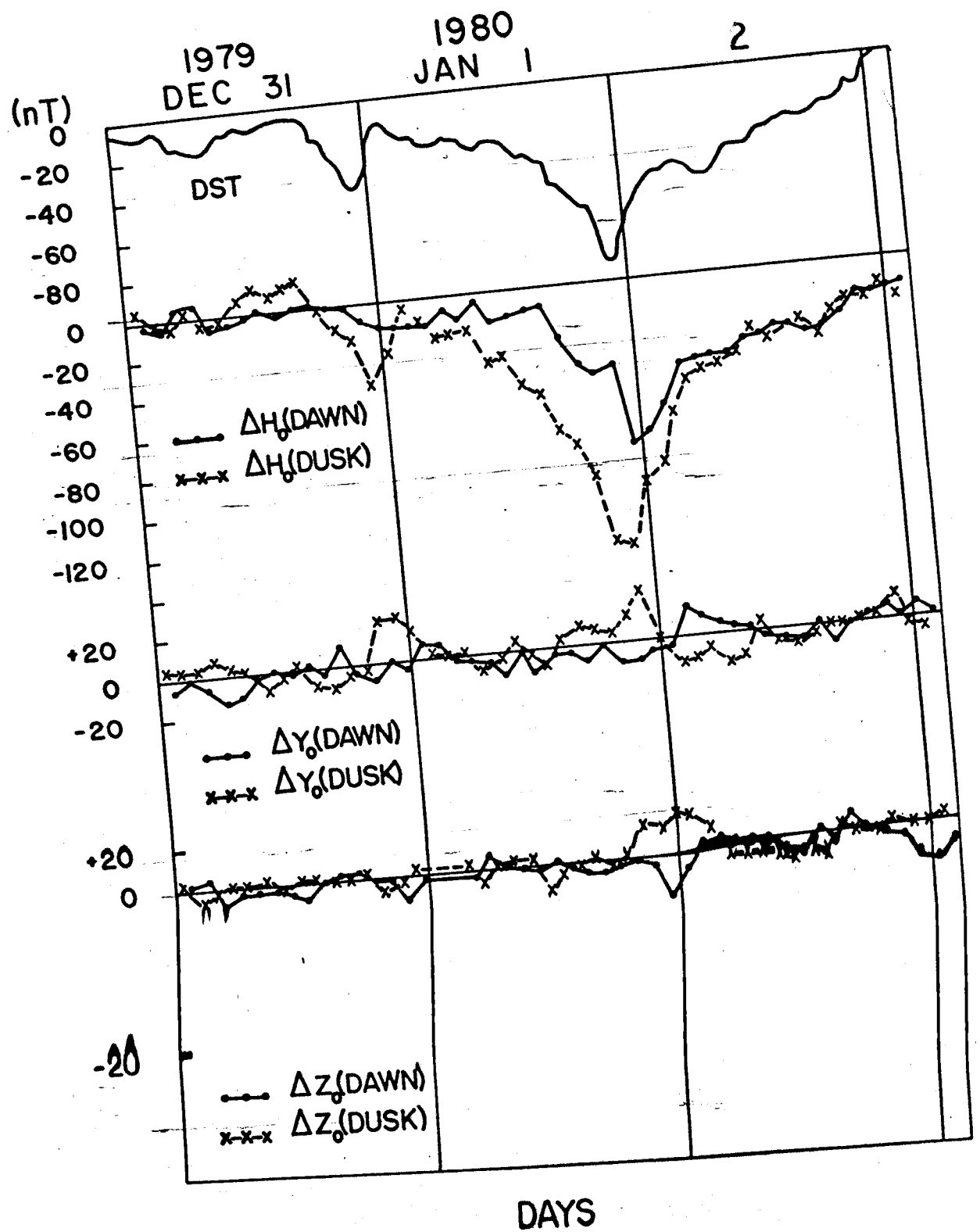


Fig. 13 - Plots of Dst and the base-level-corrected values of ΔH_0 , ΔY_0 , ΔZ_0 for Dawn (dots with full lines) and Dusk (dashes with crosses), for the storm period Dec. 31, 1979 - Jan. 2, 1980.

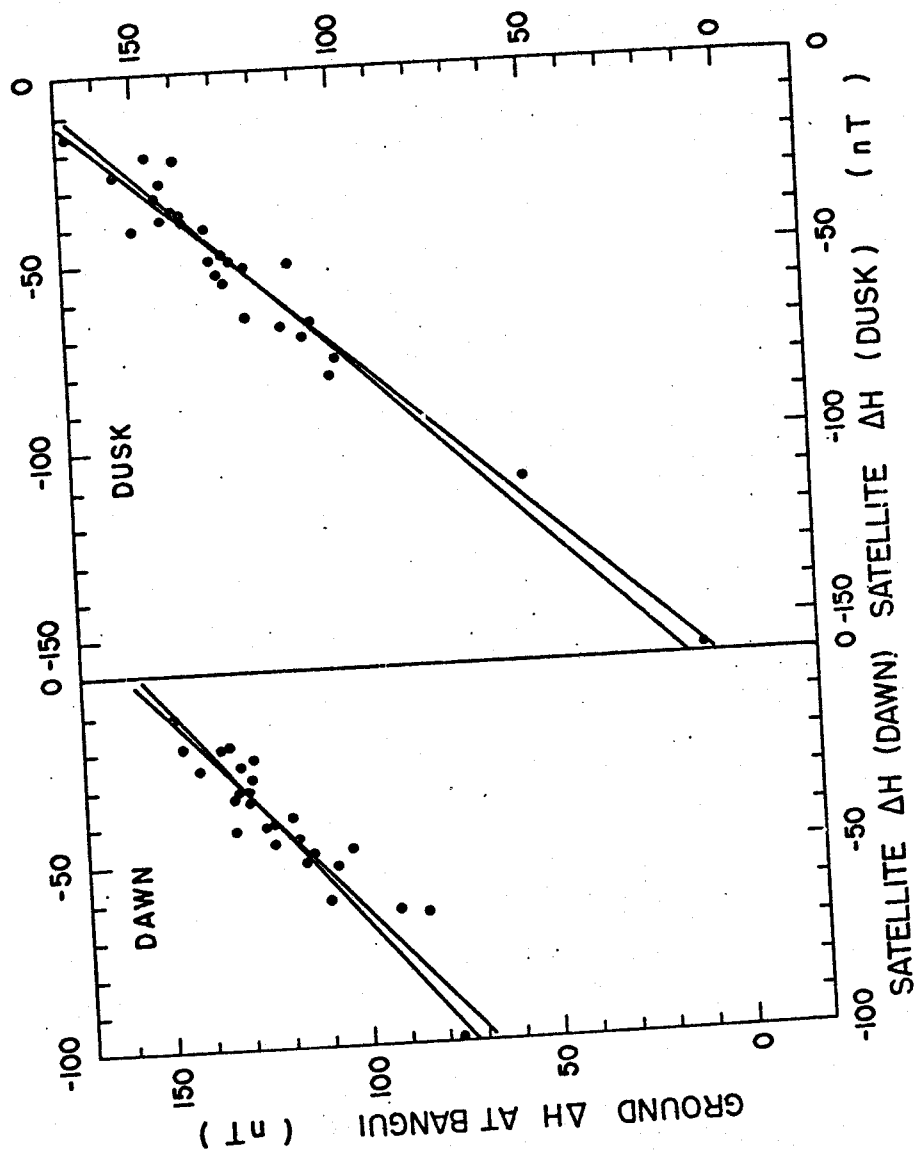


Fig. 14 - ΔH at Bangui (5°N , 19°E) versus MAGSAT ΔH_0 values at 5°N for Dawn and Dusk passes near 19°E longitude, for Nov. 3-30, 1979. Excellent correlation with regression lines of slope almost unity are indicated, implying very good parallelism between ground variations and MAGSAT variations.

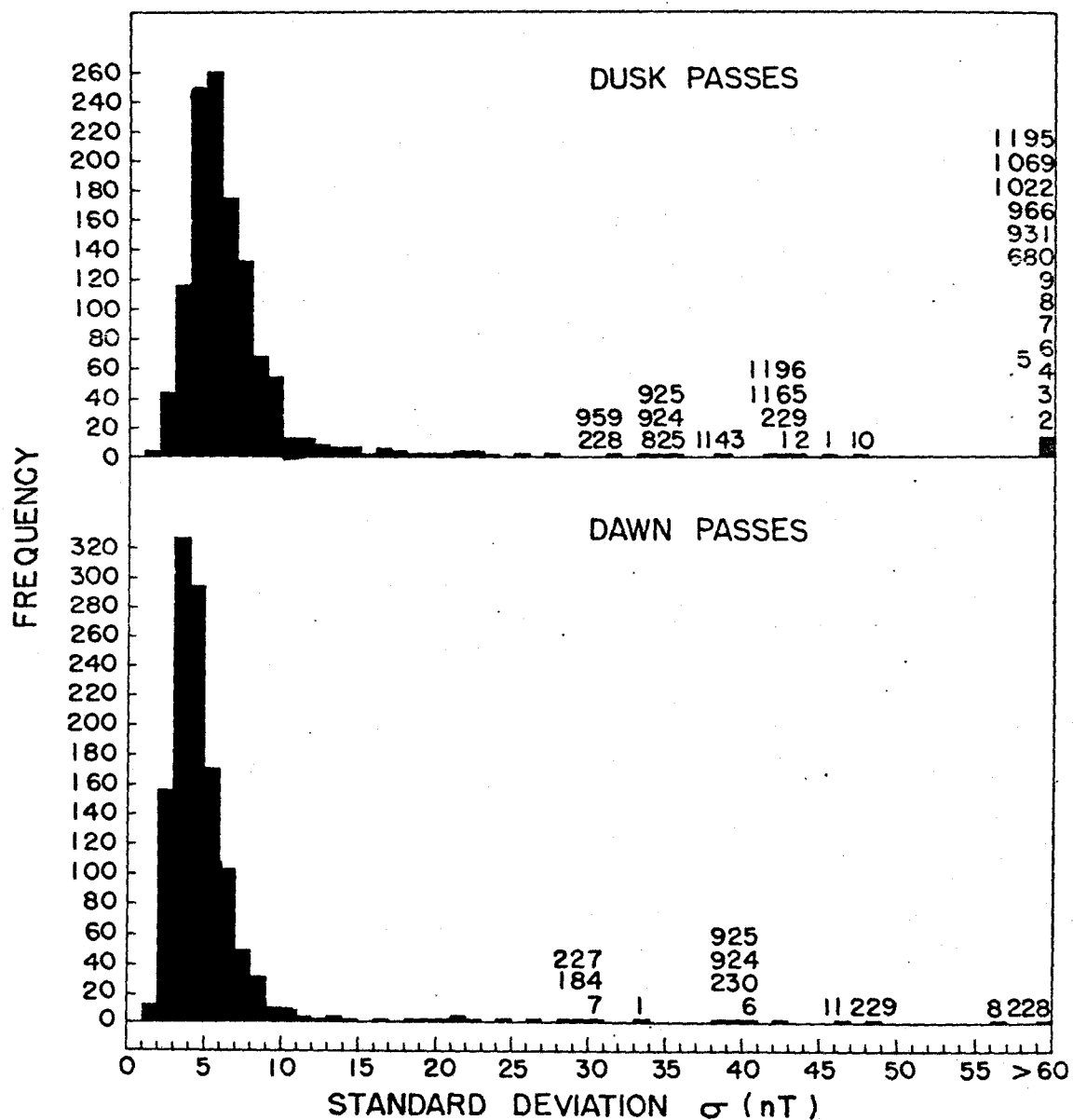


Fig. 15 - Frequency distribution of the Standard Deviation (σ) for about 1200 Dusk passes (upper half) and Dawn passes (lower half). Pass numbers for abnormally large σ are indicated.

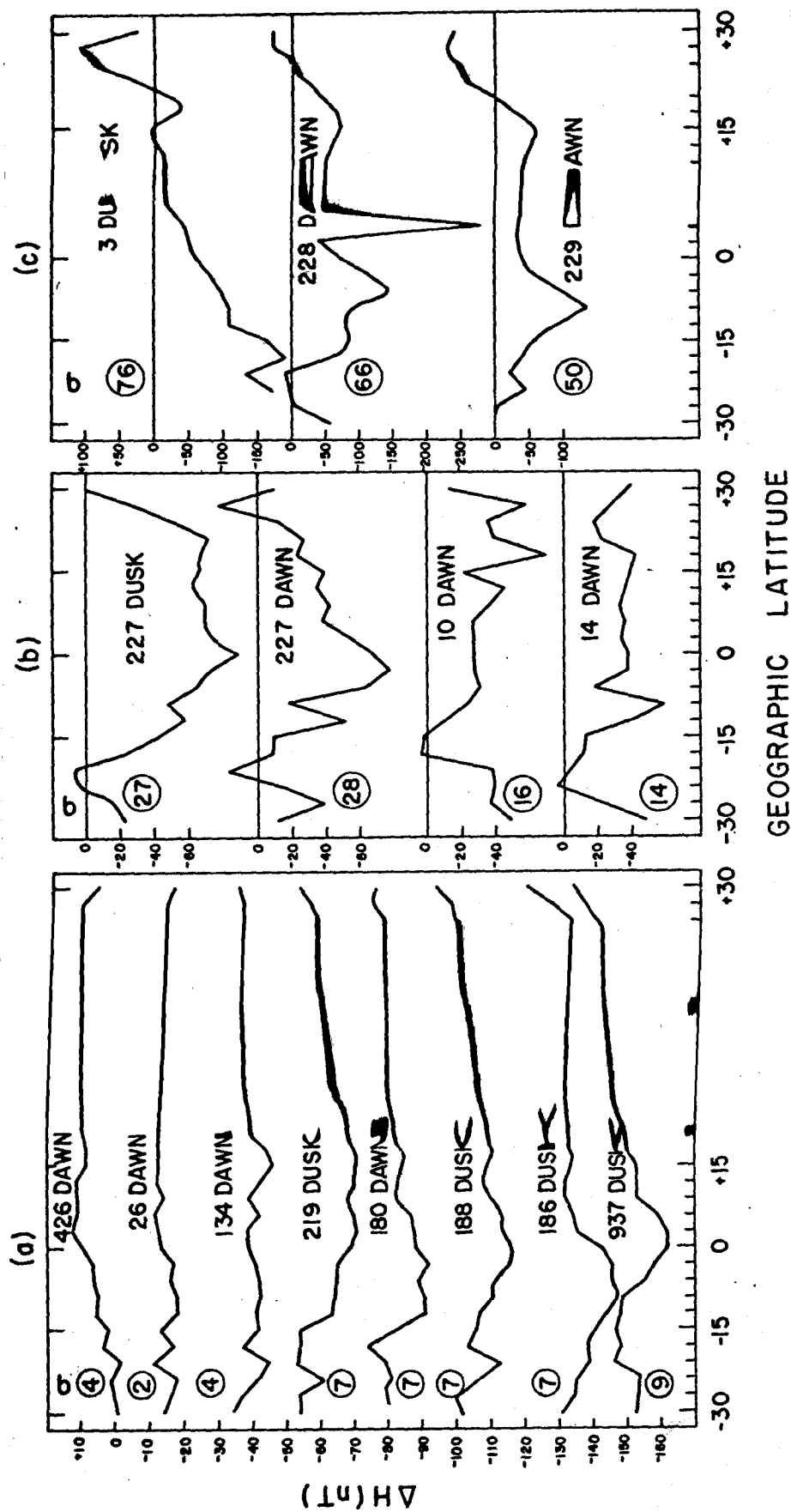


Fig. 16 - The latitudinal distribution of ΔH for a few selected passes with ΔH less than 10 nT, between 10 nT and 30 nT, and exceeding 30 nT. Labels indicate Pass number and LT (Dusk or Dawn)

Table 1: U.T., Longitude and ΔH at equatorial crossing, as well as other parameters for passes 154-169 on Nov. 12, 1979 (Julian days 44189).

Pass No	UT	DUSK swing		DAWN swing		Dst	Complete set with Manipulated values				Average of DUSK ΔH_0 and DAWN ΔH_0	Difference DUSK ΔH_0 minus DAWN ΔH_0
		Long.	ΔH_0	Long.	ΔH_0		DUSK swing		DAWN swing			
							Long.	ΔH_0	Long.	ΔH_0		
154	0.0	- 96 ⁰	- 27	-	-	+ 1	- 96 ⁰	- 27				
154	0.8	-	-	+ 73 ⁰	- 15	+ 1	- 108 ⁰	- 29	+ 73 ⁰	- 15	- 22	- 14
155	1.6	- 119 ⁰	- 30	-	-	+ 1	- 119 ⁰	- 30	+ 61 ⁰	- 17	- 24	- 13
155	2.4	-	-	+ 49 ⁰	- 18	- 1	- 132 ⁰	- 29	+ 49 ⁰	- 18	- 24	- 11
156	3.3	- 143 ⁰	- 27	-	-	+ 2	- 143 ⁰	- 27	+ 38 ⁰	- 24	- 26	- 3
156	4.1	-	-	+ 26 ⁰	- 30	+ 7	- 155 ⁰	- 26	+ 26 ⁰	- 30	- 28	+ 4
157	5.0	- 166 ⁰	- 24	-	-	+ 9	- 166 ⁰	- 24	+ 15 ⁰	- 26	- 25	+ 2
157	5.9	-	-	+ 3 ⁰	- 21	0	- 178 ⁰	- 24	+ 3 ⁰	- 21	- 23	- 3
158	6.8	+ 171 ⁰	- 23	-	-	0	+ 171 ⁰	- 23	+ 9 ⁰	- 23	- 23	0
158	7.6	-	-	- 21 ⁰	- 24	+ 1	+ 159 ⁰	- 33	- 21 ⁰	- 24	- 29	- 9
159	8.4	+ 147 ⁰	- 42	-	-	0	+ 147 ⁰	- 42	- 33 ⁰	- 16	- 29	- 26
159	9.2	-	-	- 44 ⁰	- 8	0	+ 136 ⁰	- 41	- 44 ⁰	- 8	- 25	- 33
160	10.0	+ 124 ⁰	- 40	-	-	0	+ 124 ⁰	- 40	- 56 ⁰	- 17	- 29	- 23
160	10.7	-	-	- 68 ⁰	- 25	+ 13	+ 112 ⁰	- 39	- 68 ⁰	- 25	- 32	- 14
161	11.4	+ 100 ⁰	- 37	-	-	+ 5	+ 100 ⁰	- 37	- 80 ⁰	- 24	- 31	- 13
161	12.4	-	-	- 91 ⁰	- 23	+ 6	+ 89 ⁰	- 41	- 91 ⁰	- 23	- 32	- 18
162	12.9	+ 77 ⁰	- 44	-	-	+ 6	+ 77 ⁰	- 44	- 103 ⁰	- 25	- 35	- 19
162	13.9	-	-	- 115 ⁰	- 26	+ 1	+ 65 ⁰	- 41	- 115 ⁰	- 26	- 34	- 15
163	14.4	+ 53 ⁰	- 37	-	-	- 1	+ 53 ⁰	- 37	- 127 ⁰	- 25	- 31	- 12
163	15.2	-	-	- 138 ⁰	- 24	- 3	+ 42 ⁰	- 39	- 138 ⁰	- 24	- 32	- 15
164	15.9	+ 30 ⁰	- 40	-	-	- 3	+ 30 ⁰	- 40	- 150 ⁰	- 25	- 33	- 15
164	16.9	-	-	- 161 ⁰	- 25	- 3	+ 19 ⁰	- 46	- 161 ⁰	- 25	- 36	- 21
165	17.5	+ 7 ⁰	- 51	-	-	0	+ 7 ⁰	- 51	- 173 ⁰	- 28	- 40	- 23
165	18.2	-	-	+ 175 ⁰	- 31	+ 4	- 5 ⁰	- 39	+ 175 ⁰	- 31	- 35	- 8
166	19.0	+ 17 ⁰	- 26	-	-	+ 4	- 17 ⁰	- 26	+ 164 ⁰	- 26	- 26	0
166	19.7	-	-	+ 152 ⁰	- 21	+ 4	- 29 ⁰	- 24	+ 152 ⁰	- 21	- 23	- 3
167	20.5	- 40 ⁰	- 22	-	-	1	- 40 ⁰	- 22	+ 140 ⁰	- 25	- 24	+ 3
167	21.2	-	-	+ 128 ⁰	- 29	- 9	- 52 ⁰	- 25	+ 128 ⁰	- 29	- 27	+ 4
168	21.9	- 64 ⁰	- 27	-	-	- 9	- 64 ⁰	- 27	+ 117 ⁰	- 27	- 27	0
168	22.7	-	-	+ 105 ⁰	- 25	- 9	- 76 ⁰	- 28	+ 105 ⁰	- 25	- 27	- 3
169	23.4	- 87 ⁰	- 29	-	-	- 6	- 87 ⁰	- 29				

Table 2: $\Delta\bar{H}_0$, $\Delta\bar{Y}_0$, $\Delta\bar{Z}_0$ (with their standard errors) and their
Average = (Value at Dusk + Value at Dawn)/2 and Difference =
(Value at Dusk minus Value at Dawn) for successive 5°
longitude intervals.

Longitude group	DUSK						DAWN						Average (Dusk + Dawn)/2			Difference (Dusk - Dawn)		
	$\Delta\bar{H}_0$	$\sigma\bar{H}_0$	$\Delta\bar{Y}_0$	$\sigma\bar{Y}_0$	$\Delta\bar{Z}_0$	$\sigma\bar{Z}_0$	$\Delta\bar{H}_0$	$\sigma\bar{H}_0$	$\Delta\bar{Y}_0$	$\sigma\bar{Y}_0$	$\Delta\bar{Z}_0$	$\sigma\bar{Z}_0$	$\Delta\bar{H}_0$	$\sigma\bar{H}_0$	$\Delta\bar{Y}_0$	$\sigma\bar{Y}_0$	$\Delta\bar{Z}_0$	$\sigma\bar{Z}_0$
- 180, - 175	- 36	± 2	+ 6	± 1	- 6	± 1	- 21	± 2	- 18	± 3	- 10	± 1	- 29	- 6	- 8	- 15	+ 24	+ 4
- 175, - 170	- 35	± 2	+ 7	± 2	- 4	± 1	- 18	± 1	- 20	± 2	- 12	± 1	- 27	- 7	- 8	- 17	+ 27	+ 8
- 170, - 165	- 35	± 1	+ 4	± 2	- 6	± 1	- 15	± 2	- 19	± 2	- 8	± 1	- 22	- 7	- 7	- 20	+ 23	+ 2
- 165, - 160	- 30	± 2	+ 3	± 2	- 8	± 1	- 17	± 2	- 26	± 4	- 10	± 1	- 24	- 12	- 9	- 13	+ 29	+ 2
- 160, - 155	- 28	± 2	+ 5	± 3	- 9	± 2	- 11	± 1	- 14	± 2	- 10	± 1	- 20	- 5	- 10	- 17	+ 19	+ 1
- 155, - 150	- 27	± 3	+ 6	± 2	- 5	± 1	- 10	± 1	- 14	± 2	- 5	± 1	- 19	- 4	- 5	- 17	+ 20	0
- 150, - 145	- 28	± 2	+ 7	± 2	- 5	± 1	- 15	± 1	- 16	± 2	- 1	± 1	- 22	- 5	- 3	- 13	+ 23	- 4
- 145, - 140	- 32	± 2	+ 1	± 2	- 4	± 1	- 15	± 2	- 14	± 3	- 5	± 1	- 24	- 7	- 5	- 17	+ 15	+ 1
- 140, - 135	- 33	± 2	0	± 1	- 8	± 1	- 16	± 1	- 18	± 3	- 6	± 1	- 25	- 9	- 7	- 17	+ 18	- 2
- 135, - 130	- 33	± 2	0	± 2	- 12	± 1	- 15	± 2	- 12	± 2	- 9	± 1	- 24	- 6	- 11	- 18	+ 12	- 3
- 130, - 125	- 30	± 2	+ 2	± 2	- 9	± 1	- 18	± 1	- 10	± 3	- 1	± 1	- 24	- 4	- 5	- 12	+ 12	- 8
- 125, - 120	- 32	± 2	+ 5	± 2	- 7	± 1	- 18	± 1	- 12	± 1	- 2	± 1	- 25	- 4	- 5	- 14	+ 17	- 5
- 120, - 115	- 38	± 3	- 4	± 2	- 4	± 1	- 22	± 1	- 14	± 3	- 2	± 1	- 30	- 9	- 3	- 16	+ 10	- 2
- 115, - 110	- 37	± 2	- 5	± 2	- 8	± 2	- 23	± 2	- 14	± 2	- 5	± 1	- 30	- 10	- 7	- 14	+ 9	- 3
- 110, - 105	- 38	± 2	- 11	± 1	- 17	± 2	- 23	± 2	- 11	± 2	- 10	± 1	- 31	- 11	- 14	- 15	0	- 7
- 105, - 100	- 36	± 3	- 2	± 2	- 22	± 1	- 22	± 2	- 7	± 2	- 15	± 1	- 29	- 5	- 19	- 14	+ 5	- 7
- 100, - 95	- 39	± 2	+ 2	± 1	- 21	± 1	- 24	± 1	- 1	± 1	- 13	± 1	- 32	+ 1	- 17	- 15	+ 3	- 8
- 95, - 90	- 34	± 1	+ 3	± 1	- 15	± 1	- 24	± 2	+ 5	± 2	- 7	± 1	- 29	+ 4	- 11	- 10	- 2	- 8
- 90, - 85	- 35	± 2	0	± 3	- 12	± 1	- 28	± 1	0	± 2	0	± 1	- 32	0	- 6	- 7	0	- 12
- 85, - 80	- 38	± 2	- 6	± 2	- 11	± 1	- 28	± 1	- 1	± 2	- 3	± 1	- 33	- 4	- 7	- 10	- 5	- 8
- 80, - 75	- 33	± 2	- 1	± 3	- 16	± 1	- 25	± 1	+ 2	± 3	- 6	± 1	- 29	+ 1	- 11	- 8	- 3	- 10
- 75, - 70	- 32	± 3	- 5	± 2	- 16	± 1	- 25	± 2	+ 4	± 3	- 6	± 2	- 29	- 1	- 11	- 7	- 9	- 10
- 70, - 65	- 30	± 2	0	± 2	- 10	± 2	- 19	± 2	+ 11	± 2	- 5	± 1	- 25	+ 6	- 8	- 11	- 11	- 5
- 65, - 60	- 29	± 3	+ 1	± 4	- 11	± 2	- 21	± 1	+ 11	± 2	- 4	± 1	- 25	+ 6	- 8	- 8	- 10	- 7
- 60, - 55	- 26	± 3	- 1	± 3	- 9	± 1	- 19	± 2	+ 10	± 2	- 1	± 1	- 23	+ 5	- 5	- 7	- 11	- 8
- 55, - 50	- 28	± 2	- 1	± 4	- 6	± 2	- 15	± 2	+ 4	± 2	- 3	± 1	- 22	+ 2	- 5	- 11	- 5	- 3
- 50, - 45	- 29	± 2	0	± 3	- 9	± 1	- 13	± 3	+ 4	± 3	- 6	± 1	- 21	+ 2	- 8	- 16	- 4	- 3
- 45, - 40	- 29	± 3	+ 3	± 3	- 7	± 1	- 15	± 2	+ 8	± 2	- 2	± 1	- 22	+ 6	- 5	- 14	- 5	- 5
- 40, - 35	- 35	± 3	+ 12	± 3	- 2	± 1	- 17	± 2	+ 8	± 2	- 1	± 1	- 26	+ 10	- 2	- 18	+ 4	- 1
- 35, - 30	- 32	± 4	+ 12	± 2	0	± 1	- 15	± 2	+ 4	± 2	- 6	± 1	- 24	+ 8	- 3	- 17	+ 8	+ 6
- 30, - 25	- 32	± 2	+ 18	± 2	- 1	± 1	- 20	± 2	+ 5	± 2	- 9	± 1	- 26	+ 12	- 5	- 12	+ 13	+ 8
- 25, - 20	- 34	± 4	+ 22	± 2	+ 1	± 2	- 22	± 2	+ 7	± 2	- 10	± 1	- 28	+ 15	- 5	- 12	+ 15	+ 11
- 20, - 15	- 34	± 4	+ 27	± 2	+ 5	± 1	- 25	± 2	+ 6	± 1	- 6	± 1	- 30	+ 17	- 1	- 9	+ 21	+ 11
- 15, - 10	- 29	± 3	+ 21	± 2	+ 8	± 1	- 25	± 1	+ 8	± 2	- 5	± 2	- 27	+ 15	+ 2	- 4	+ 13	+ 13
- 10, - 5	- 35	± 3	+ 14	± 3	+ 8	± 1	- 22	± 1	0	± 2	- 4	± 1	- 29	+ 7	+ 2	- 13	+ 14	+ 12
- 5, - 0	- 37	± 3	+ 16	± 1	+ 4	± 1	- 24	± 2	- 3	± 2	- 5	± 1	- 31	+ 7	- 1	- 13	+ 19	+ 9

(continued)

Table 2: Continued

Longitude group	DUSK						DAWN						Average (Dusk + Dawn)/2			Difference (Dusk - Dawn)		
	ΔH_0	σH_0	ΔV_0	σV_0	ΔZ_0	σZ_0	ΔH_0	σH_0	ΔV_0	σV_0	ΔZ_0	σZ_0	ΔH_0	ΔV_0	ΔZ_0	ΔH_0	ΔV_0	ΔZ_0
0, 5	-40	± 5	+17	± 3	+2	± 1	-26	± 2	+1	± 2	-8	± 1	-33	+9	-3	-14	+16	+10
5, 10	-41	± 2	+18	± 2	+6	± 1	-31	± 2	+5	± 1	-7	± 1	-36	+12	-1	-10	+13	+13
10, 15	-37	± 3	+16	± 2	+14	± 1	-28	± 2	+4	± 2	0	± 1	-33	+10	+7	-9	+12	+14
15, 20	-28	± 3	+8	± 2	+17	± 2	-19	± 2	-3	± 1	+3	± 1	-24	+3	+10	-9	+11	+14
20, 25	-24	± 3	+6	± 1	+10	± 1	-17	± 3	-5	± 1	+2	± 3	-21	+1	+6	-7	+11	+8
25, 30	-34	± 4	+11	± 2	+6	± 1	-23	± 2	-3	± 1	-9	± 1	-29	+4	-2	-11	+14	+15
30, 35	-34	± 3	+13	± 2	0	± 1	-24	± 1	-1	± 2	-8	± 1	-29	+6	-4	-10	+14	+8
35, 40	-37	± 3	+18	± 2	+3	± 1	-26	± 2	+1	± 2	-5	± 1	-32	+10	-1	-11	+17	+8
40, 45	-34	± 3	+14	± 2	+8	± 1	-25	± 2	-2	± 1	-2	± 1	-30	+6	+3	-9	+16	+10
45, 50	-36	± 4	+13	± 2	+4	± 1	-24	± 2	-5	± 1	-6	± 1	-30	+4	-1	-12	+18	+10
50, 55	-37	± 4	+19	± 3	0	± 1	-25	± 2	-4	± 1	-8	± 1	-31	+8	-4	-12	+23	+8
55, 60	-38	± 2	+17	± 1	+4	± 1	-25	± 4	-3	± 2	-8	± 2	-32	+7	-2	-13	+20	+12
60, 65	-41	± 6	+17	± 2	0	± 1	-26	± 2	-5	± 1	-8	± 1	-34	+6	-4	-15	+22	+8
65, 70	-35	± 2	+16	± 2	0	± 1	-28	± 2	-9	± 2	-11	± 1	-32	+4	-6	-7	+25	+11
70, 75	-38	± 3	+12	± 2	-3	± 2	-23	± 2	-8	± 1	-13	± 1	-31	+2	-8	-15	+20	+10
75, 80	-37	± 2	+13	± 2	-9	± 1	-24	± 3	-9	± 1	-17	± 1	-31	+2	-13	-13	+22	+8
80, 85	-37	± 2	+19	± 1	-8	± 1	-25	± 1	-6	± 2	-18	± 1	-31	+7	-13	-12	+25	+10
85, 90	-36	± 4	+17	± 2	-1	± 2	-21	± 2	-4	± 4	-15	± 1	-29	+7	-8	-15	+21	+14
90, 95	-35	± 3	+13	± 2	-2	± 2	-19	± 3	-5	± 1	-10	± 1	-27	+4	-6	-16	+18	+8
95, 100	-33	± 2	+10	± 1	-1	± 2	-26	± 1	-10	± 2	-15	± 1	-30	0	-8	-7	+20	+14
100, 105	-29	± 2	+13	± 2	-6	± 1	-24	± 2	-9	± 2	-17	± 2	-27	+2	-12	-5	+22	+11
105, 110	-33	± 2	+12	± 2	-2	± 2	-23	± 1	-8	± 1	-16	± 1	-28	+2	-9	-10	+20	+14
110, 115	-29	± 2	+13	± 2	-5	± 1	-19	± 2	-6	± 1	-17	± 2	-24	+4	-11	-10	+19	+12
115, 120	-31	± 2	+18	± 2	-6	± 1	-21	± 1	-6	± 1	-15	± 1	-26	+6	-11	-10	+24	+9
120, 125	-34	± 2	+21	± 2	-4	± 1	-26	± 2	-1	± 2	-12	± 3	-30	+10	-8	-8	+22	+8
125, 130	-37	± 2	+21	± 2	+3	± 2	-27	± 3	-5	± 2	-9	± 2	-32	+8	-3	-10	+26	+12
130, 135	-35	± 2	+19	± 2	+5	± 2	-24	± 2	-6	± 2	-9	± 1	-30	+7	-2	-11	+25	+14
135, 140	-34	± 2	+22	± 2	+5	± 1	-21	± 2	-9	± 2	-9	± 1	-27	+7	-2	-13	+31	+14
140, 145	-30	± 2	+14	± 2	+3	± 1	-22	± 1	-8	± 2	-10	± 1	-26	+3	-4	-8	+22	+13
145, 150	-36	± 2	+15	± 2	0	± 1	-27	± 2	-12	± 2	-13	± 1	-32	+2	-7	-9	+27	+13
150, 155	-39	± 2	+14	± 2	-6	± 2	-26	± 2	-12	± 3	-16	± 1	-33	+1	-11	-13	+26	+10
155, 160	-34	± 2	+20	± 2	-8	± 1	-25	± 1	-7	± 1	-17	± 1	-30	+7	-13	-9	+27	+9
160, 165	-30	± 2	+23	± 2	-2	± 2	-25	± 2	-3	± 3	-11	± 1	-28	+10	-7	-5	+26	+9
165, 170	-35	± 2	+16	± 1	-2	± 1	-22	± 2	-13	± 2	-10	± 1	-29	+2	-6	-13	+29	+8
170, 175	-34	± 1	+12	± 1	-5	± 1	-23	± 2	-15	± 2	-13	± 1	-29	-2	-9	-11	+27	+8
175, 180	-37	± 2	+10	± 2	-4	± 2	-23	± 1	-18	± 2	-11	± 1	-30	-4	-8	-14	+28	+7

(Conclusion)

Table 3: List and details of stations and results (correlation coefficients and slopes with errors) of a correlation analysis for a linear fit $Y = mX + c$, where Y = Independent variable, X = Dependent variable, m = slope.

Station	Geographic		DAWN PASSES (0600)				DUSK PASSES (1800)			
			Y = Satellite X = Ground		Y = Ground X = Satellite		Y = Satellite X = Ground		Y = Ground X = Satellite	
			Corr. Coeff.	Slope(m)	Corr. Coeff.	Slope(m)	Corr. Coeff.	Slope(m)	Corr. Coeff.	Slope(m)
TSUMEB	19.2°S	17.7°E	+ 0.93	1.05 ± 0.08	+ 0.93	0.82 ± 0.07	+ 0.99	0.97 ± 0.03	+ 0.99	1.00 ± 0.03
BANGUI	4.6°N	18.6°E	+ 0.93	1.07 ± 0.08	+ 0.93	0.81 ± 0.06	+ 0.97	0.91 ± 0.04	+ 0.97	1.04 ± 0.05
HERMANUS	34.4°S	19.2°E	+ 0.78	0.85 ± 0.14	+ 0.78	0.71 ± 0.11	+ 0.97	1.10 ± 0.06	+ 0.97	0.85 ± 0.04
GNANGARA	31.8°S	116.0°E	+ 0.85	0.84 ± 0.10	+ 0.85	0.87 ± 0.11	+ 0.81	0.97 ± 0.14	+ 0.81	0.67 ± 0.10
MUNTINLUPA	14.4°N	121.0°E	+ 0.95	1.07 ± 0.07	+ 0.95	0.84 ± 0.06	+ 0.92	0.94 ± 0.08	+ 0.92	0.91 ± 0.07
LUNPING	25.2°N	121.2°E	+ 0.97	0.99 ± 0.05	+ 0.97	0.95 ± 0.05	+ 0.97	0.90 ± 0.05	+ 0.97	1.05 ± 0.05
GUAM	13.6°N	144.9°E	+ 0.97	0.95 ± 0.05	+ 0.97	0.99 ± 0.05	+ 0.98	1.01 ± 0.04	+ 0.98	0.95 ± 0.04
PORT MORESBY	9.4°S	147.1°E	+ 0.96	1.00 ± 0.06	+ 0.96	0.92 ± 0.05	+ 0.97	0.92 ± 0.05	+ 0.97	1.02 ± 0.05
HONOLULU	21.3°N	158.1°W	+ 0.90	0.98 ± 0.09	+ 0.90	0.82 ± 0.08	+ 0.94	1.03 ± 0.08	+ 0.94	0.86 ± 0.06
TAHITI	17.7°S	149.3°W	+ 0.95	0.86 ± 0.05	+ 0.95	1.05 ± 0.07	+ 0.96	0.99 ± 0.06	+ 0.96	0.93 ± 0.05
TUCSON	32.0°N	111.5°W	+ 0.94	0.90 ± 0.06	+ 0.94	0.98 ± 0.07	+ 0.95	0.99 ± 0.07	+ 0.95	0.91 ± 0.06
HUANCAYO	12.1°S	75.3°W	+ 0.92	1.02 ± 0.08	+ 0.92	0.83 ± 0.07	+ 0.92	0.94 ± 0.08	+ 0.92	0.90 ± 0.08
FUQUENE	5.5°N	73.8°W	+ 0.94	1.03 ± 0.08	+ 0.94	0.85 ± 0.06	+ 0.92	0.99 ± 0.08	+ 0.92	0.87 ± 0.07
SAN JUAN	18.1°N	66.2°W	+ 0.96	0.84 ± 0.05	+ 0.96	1.10 ± 0.06	+ 0.95	0.93 ± 0.06	+ 0.95	0.97 ± 0.07
VASSOURAS	22.4°S	43.6°W	+ 0.88	0.73 ± 0.08	+ 0.88	1.06 ± 0.11	+ 0.96	0.89 ± 0.05	+ 0.96	1.03 ± 0.06
M'BOUR	14.4°N	17.0°W	+ 0.97	0.95 ± 0.05	+ 0.97	0.99 ± 0.05	+ 0.98	0.99 ± 0.04	+ 0.98	0.97 ± 0.04
Average				0.946 ± 0.015		0.912 ± 0.015		0.967 ± 0.015		0.933 ± 0.015

0.933 ± 0.015

Table 4: Frequency of passes

σ (nT)	Dawn	Dusk
0 to 1	0	0
1 to 2	12	3
2 to 3	156	44
3 to 4	326	115
4 to 5	293	247
5 to 6	170	260
6 to 7	102	173
7 to 8	48	131
8 to 9	30	67
9 to 10	9	54
10 to 11	8	12
11 to 12	3	11
12 to 13	2	8
13 to 14	3	6
14 to 15	1	7
15 to 16	0	1
16 to 17	1	5
17 to 18	0	4
18 to 19	1	3
19 to 20	1	1
0 to 5	787	409
5 to 10	359	685
10 to 15	17	44
15 to 20	3	14
20 to 25	9	6
25 to 30	3	2
30 to 40	4	6
40 to 50	4	6
50 to 60	1	0
> 60	1	14
0 to 10	1146	1094
> 10	42	92
Total	1188	1186

Table 5: Passes which are probably faulty

σ (nT)	Dawn Pass numbers	Count	Dusk Pass numbers	Count
> 60	228,	1	2, 3, 4, 5, 6, 7, 8, 9, 680, 931, 966, 1022, 1069, 1195	14
50 to 60	8,	1		0
40 to 50	11, 229, 230, 924	4	1, 10, 12, 229, 1165, 1196	6
30 to 40	1, 6, 7, 925	4	228, 852, 924, 925, 959, 1143	6
25 to 30	9, 184, 227	3	178, 227	2
20 to 25	3, 5, 12, 13, 181, 369, 453, 554, 845	9	230, 795, 883, 1153, 1154, 1201	6
15 to 20	10, 195, 846	3	11, 13, 175, 176, 177, 399, 824, 849, 884 899, 939, 940, 972, 1145	14
12 to 15	2, 4, 14, 436, 533, 694	6	97, 140, 179, 185, 200, 231, 339, 344 654, 776, 781, 863, 906, 909, 929, 930 938, 994, 1133, 1173, 1176	21
10 to 12	100, 121, 177, 344, 346, 560 822, 939, 940, 955, 1091	11	62, 88, 100, 108, 138, 139, 198, 349 415, 436, 452, 508, 668, 683, 684, 775 829, 846, 941, 981, 1002, 1048, 1124	23
> 10		42		92